Quantifying onshore salt deposits and their potential for hydrogen energy storage in Australia

Citation for published version:
Aftab, A, Hassanpouryouzband, A, Naderi, H, Xie, Q & Sarmadivaleh, M 2023, 'Quantifying onshore salt deposits and their potential for hydrogen energy storage in Australia', *Journal of Energy Storage*, vol. 65, 107252. https://doi.org/10.1016/j.est.2023.107252

Digital Object Identifier (DOI):
10.1016/j.est.2023.107252

Link:
Link to publication record in Edinburgh Research Explorer

Document Version:
Peer reviewed version

Published In:
Journal of Energy Storage

Quantifying onshore salt deposits and their potential for hydrogen energy storage in Australia

Adnan Aftab[1,2*], Aliakbar Hassanpouryouzband[2], Hamed Naderi[3], Quan Xie[1], Mohammad Sarmadivaleh[1*]

[1]School of Western Australia School of Mines: Minerals, Energy and Chemical Engineering, Curtin University, Kensington, Australia.

[2]School of Geosciences, University of Edinburgh, Grant Institute, West Main Road, 7 Edinburgh EH9 3FE, U.K.

[3]Sarvak Azar Engineering and Development Company (SAED Co.), Tehran, Iran

Corresponding Emails: adnan.aftab@postgrad.curtin.edu.au; mohammad.sarmadivaleh@curtin.edu.au

Abstract

Hydrogen energy will remarkably aid the global energy transition from fossil fuels to renewables. Hydrogen is the lightest molecule. It requires large volume storage facilities only found in geological formations. Salt caverns are a potential geo-storage medium that has been used in practice at a commercial scale. In Australia, several basins, i.e., Advalae, Carnarvon, Amadeus, Officer, and Canning, have been identified with notable salt deposits. The feasibility and potential of storing hydrogen in these salts have yet to be determined by geology, salt thickness, or salt type data. Here, we identified potential hydrogen storage sites. Additionally, hydrogen storage volume was estimated in Mallowa and Minjoo salts (Carribuddy salts: ~95 % halite and ~1 % anhydrite) in Willara Sub-basin, Canning Basin, Western Australia (WA). The results show a high potential for constructing salt caverns for hydrogen storage in these areas.

The geochemical data suggest the presence of Bromine (90 to 670 ppm and <150 ppm in some wells), which are favorable for the solution mining process for the development of salt caverns. Our study demonstrates that approximately 28282 onshore salt caverns (500000 m^3 each) could be constructed in the Willara Sub-basin salt in WA. The estimated number of caverns can store 14,697 PJ of hydrogen energy. The proposed site would be in the Northwest of WA, ~70 to 80 km from the Indian Ocean, with access to the shore and transportation. The estimated H_2 storage capacity in the salt caverns satisfies Australia's energy consumption (5,790 PJ in 2020-21), providing 8900 PJ of H_2 energy for export to ensure a sustainable hydrogen value chain.

Keywords: Western Australia, Canning basin, hydrogen storage, salt cavern, energy

1 Introduction

Fossil fuels release a considerable portion of greenhouse gas emissions, around 64%. These emissions significantly contribute to global warming and climate change [1-3]. The Paris agreement 2015 and COP26 2021 took global initiatives to mitigate CO_2 emissions and achieve CO_2 neutrality in the atmosphere [4]. The earth's surface was estimated to be 1 °C warmer compared to the beginning of the industrial revolution [5]. So far, more than 1260 climate acts are functional to protect against climate change around the globe.

Moreover, 100 countries have joined an alliance for net-zero emissions by 2050. Despite these efforts, it was estimated that CO_2 concentrations in the atmosphere would continuously rise to 417 ppm in 2021 [6-8]. Figure 1a illustrates that CO_2 emissions increase with the global human population. These emissions are mainly human-based due to the 85% share of fossil fuels in the global energy supply (Figure 1b). Therefore, it is vital to develop clean and sustainable energy production and storage systems [1, 9-11].

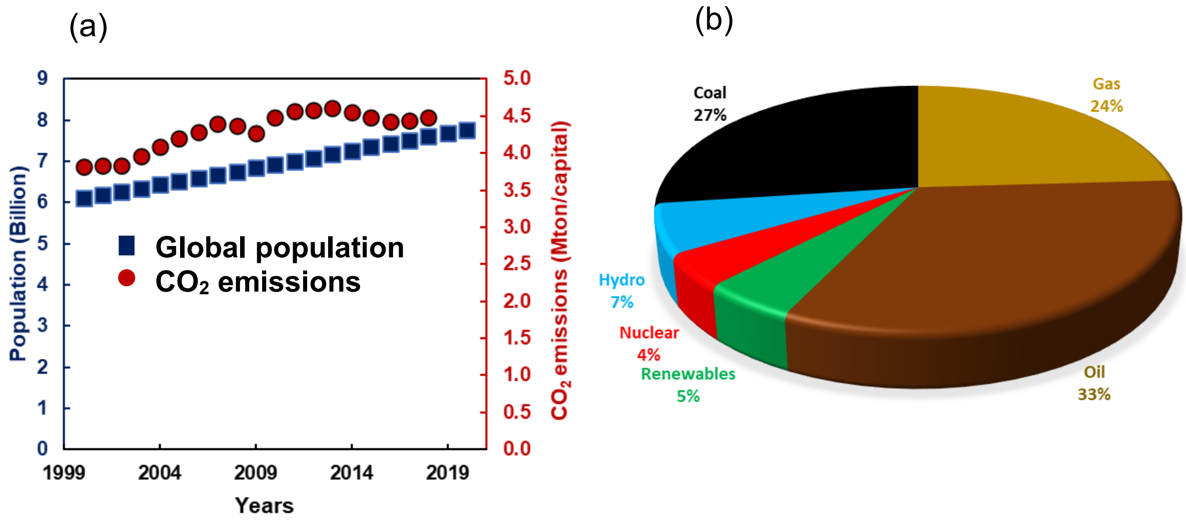

Figure 1 (a) Global population and CO_2 emissions (data taken from studies [12, 13]). (b) Renewable and non-renewable global energy utilization (data from the study [14]).

Hydrogen is a green energy carrier of the future, indispensable to climate protection [15]. To achieve a net-zero emissions scenario by 2050, European Commission, the US, China, the UK, Canada, Saudi Arabia, and Australia have visioned and aimed to develop a clean hydrogen energy ecosystem [16-19]. Sustainable energy systems (e.g., solar and wind) will be used to produce hydrogen from water via an electrocatalysis process [20, 21]. Geoscience Australia [22] predicts that Australia's resources can support the grid-scale renewable hydrogen production economy [22]. Australia's coastal areas are critical for hydrogen production through seawater electrolysis [22, 23]. However, high energy costs and the release of chlorine gas are significant issues faced during seawater electrolysis for hydrogen generation [24]. Therefore, chemists and material engineers are working on synthesizing nanocomposite-based electrodes. The electrodes consume minimum electricity (i.e., 48% lower energy than conventional electrodes), prevent chlorine problems, and thus produce clean hydrogen using seawater electrolysis [11, 23, 25-31].

Researchers [32-34] found that Australia requires large-scale energy storage solutions to widely adopt the hydrogen energy economy. Hydrogen can be stored using a variety of methods, including high-pressure cylinders (at 79.9 MPa), liquid hydrogen storage in cryogenic tanks (at 21 K), chemical hydrogen storage in metal hydrides, and physical storage in the metal-organic framework [35]. These techniques are reliable for mobile storage and industrial applications but need to address the interseasonal energy demand of the region at a massive scale [31, 36, 37]. Underground hydrogen storage (UHS) is scalable, cost-effective, and safe [38]. Depleted oil/gas reservoirs, deep saline aquifers, and salt caverns have been assessed to offer hydrogen storage. However, depleted gas reservoirs may contain methane gas which can pollute the quality of stored H_2 [39]. Additionally, deep saline aquifer rocks have a high saturation of formation water [17], which increases hydrogen trapping, thus, significant hydrogen loss during hydrogen cycling process [40]. H_2 storage in salt caverns provides multiple benefits such as flexibility (ease in injection/production cycles), vital chain link (supply for all types of clients), resilience (salt caverns conversion to H_2 storage), and safety (high tightness).

Salt domes are the ideal structure for the construction of salt caverns. The solution mining mechanism produces a salt cavern and a large amount of brine that must be disposed of in an environmentally friendly way. The generated brine can be disposed of in 3 ways: pumping into the sea, used as raw product for salt generation, and used in the chemical industry. However, the disposable cost of brine is very high [41].

Interbedded salt is another option for salt cavern construction without a salt dome. Li et al. developed a numerical model for estimating energy storage in bedded salt caverns. The findings show that insoluble layers could cause numerous difficulties during salt dissolution.

Further, the simulation results reveal uneven caverns formed due to inappropriate dissolution cycles. However, this problem can be resolved through extra leaching [42]. Liu *et al.* conducted a pre-assessment and provided a feasibility report for Jintan bedded salt mine, Jiangsu site. They show that the mine has an excellent stratigraphic trap and meets the standard selection requirement for hydrogen storage [43].

Similarly, the geography and geology of Australia provide an excellent opportunity for H_2 storage in bedded salt deposits for domestic and export purposes [44]. However, underground salt leaching mechanism and geological salt caverns' creation in the halite deposits must be better practiced in Australia [45]. Currently, there is no salt cavern exists in Australia. Seismic and salt structures data are required to develop salt caverns to store radioactive materials, anthropogenic waste, and energy products (i.e., H_2, CH_4, NH_3) in Australia [46]. Mallowa salt in the Canning basin, Western Australia, contains potential salt deposits for constructing salt caverns with a large halite unit of ~700 to 800 m [47]. This thick halite unit can be used for salt cavern construction and hydrogen storage [22, 48-51]. A thick salt layer and adequate area are prerequisites for creating salt caverns [52]. The large thickness and area of salt would ensure the cavern's integrity, prevent permeability conduits, and enhance creep stability. Halite has a high solubility in water compared to anhydrite, mudstone, and dolomite. Therefore, halite rapidly dissolves in water and does not raise undissolved layers problems during the development of the caverns [53]. Undissolved layers in the cavern can develop non-uniform salt caverns, irregular shape [54], trigger microbial activity (e.g., sulphate source/microorganism) [39] and leakages issues [55]. Salt cavern construction and fluids storage business in Australia would be a new experience. International assistance and technical expertise can be used to choose an adequate salt deposit, develop salt caverns, and improve H_2 injection/production loading [38, 45]. Overall, H_2 storage potential in salt caverns was estimated 303840 PJ in Europe [28]. Germany has 568 salt caverns potential in Lower Saxony; each has 1.368 PJ energy capacity [56]. The Netherlands [57] and Norway have 27000 PJ salt caverns hydrogen energy storage potential [58, 59]. These countries with considerable underground salt deposits could store energy fluids beyond their national energy demand as part of an energy export system [28, 60].

Feitz *et al.* [50] mapped out large-scale hydrogen production locations in Australia. A geospatial analysis of the region can provide a plan for geological hydrogen storage close to the production facility with renewable energy resources to produce green hydrogen. Salt deposits, structure, and appropriate geology, have yet to be analysed for salt cavern constructions in Australia. Therefore, further research and in-depth investigations are required to locate the targeted salt deposits for underground hydrogen storage [61]. Moreover, there is a pressing need to map out potential UHS in salt caverns with the proposed hydrogen production plants in Australia [38].

This study aims to evaluate the potential of salt deposits in Australia for hydrogen storage. This information needs to be improved in the published work. To achieve this, we have performed a concise assessment of salt deposits in different states of Australia. Targeted basins in Australia contain thick units of halite formation ranging from ~100 m to ~700 m in thickness. These halite units are essential for underground hydrogen storage subject to the geo-constraints of the region. We characterized the potential of Mallowa salt located in the Willara Sub-basin (part of Canning basin) for implementing salt cavern construction for hydrogen storage with the help of well drilling, coring, logging, isopach map, and seismic survey data. Finally, we estimated the number of salt caverns that could be constructed and the amount of hydrogen energy that could be stored in these caverns. Figure 2 displays a green and sustainable H_2 energy generation and storage process in Western Australia. Indian seashore, Telfer gas pipeline, and the Great Northern Highway are within a 100 km radius of Canning salt.

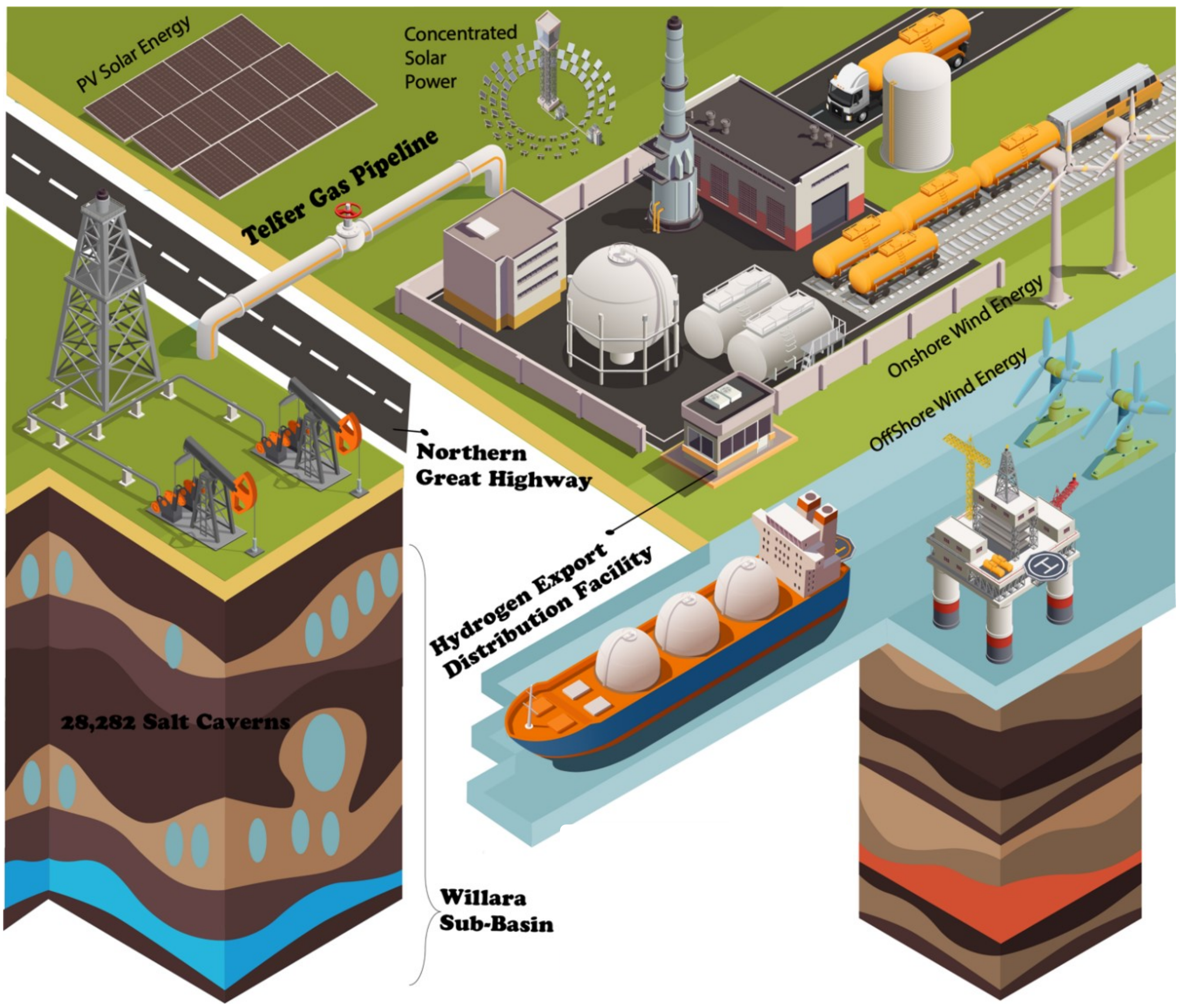

Figure 2 Illustrates proposed H_2 generation, storage, and transportation facility in Canning basin, Western Australia. Green dots in the insert Figure show wells drilled in the Canning. The wells can provide information on halite deposits for developing salt caverns.

2 Salt Basins Potential in Australia

2.1.1 Amadeus Basin

The Amadeus basin is spread over a large area of around 170000 km^2 in Central Australia. This basin mainly lies within Southern Northern Territory but expands into Western Australia [62].

Figure 3 depicts the critical factors of halite salt deposits, including export location, research facility, and underground salt deposits. The Amadeus basin is an isolated intracratonic basin in the centre of Australia. This basin consists of stratigraphy of upper Proterozoic to mid Palaeozoic exceeding 14 km thickness. More importantly, the Bitter spring formation (i.e., Gillen Member) exists at the base of Proterozoic succession, containing the earliest evaporates rock dated back to 0.8 to 0.7 Ga. These evaporates might have formed at different intervals of time when the sea level was high. The Bitter spring formation (115000 km^2) and Pinyinna beds are distributed in a vast area of around 158000 km^2 in the Amadeus basin [48, 63, 64]. More interestingly, the facies data reveal that the deposition mechanism of evaporate is cyclic and matches the deposition pattern found in other salt basins in Australia [64]. Sulphates and carbonates are found near the basin's margin [64]. Additionally, halite and possible potassium salts are formed toward the center of the basin at a later stage. Thus, the evaporite rock deposits into a shallow marine setting and salt tectonic activity start through the basin resulting in major anticline structures and salt core [65]. Further, the presence of halite is apparent in the Amadeus basin as illustrated in Figure S1 in the supplementary information. The evaporite has an average 810 m thickness in the Bitter Spring formation. Maximum evaporite thickness exceeds 2100 m below Gosses bluff impact (GBI). The average evaporite thickness beneath the Waterhouse anticline and Ooraminna anticline is 1400 m and 1800 m. These findings show the potential of the basin for the construction of salt caverns.

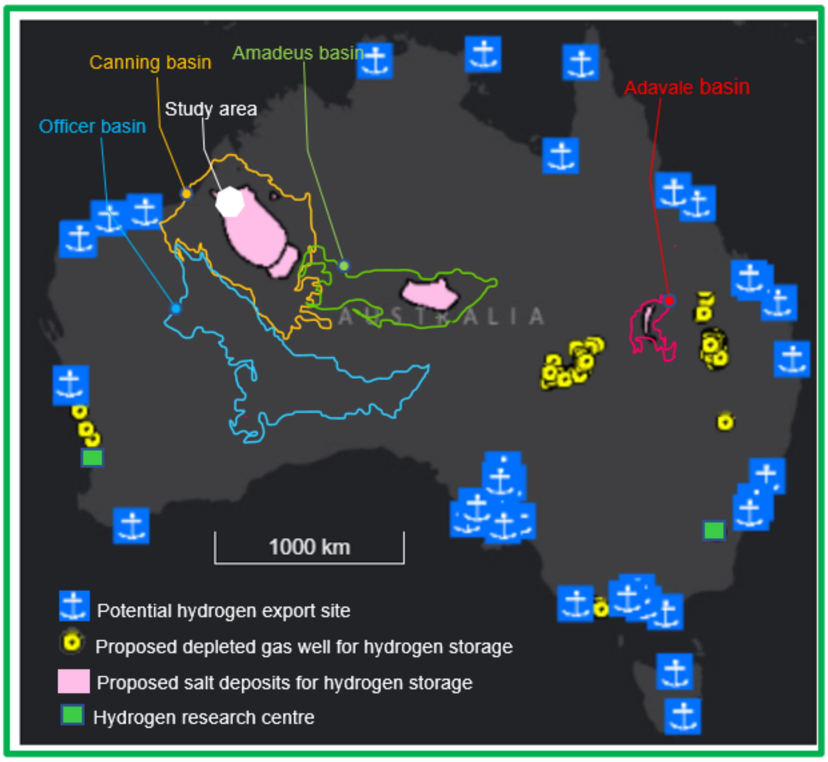

Figure 3 Advalae, Amadeus, Officer and Canning salt basins and their hydrogen generation, export and storage facilities are illustrated in Figure. This map was produced using hydrogen opportunity tool Geoscience Australia. The link for hydrogen opportunity tool [66] is provided in the supplementary information.

2.1.2 The Officer Basin

The basin contains excellent evaporate formations and salt structures (i.e., salt walls, and domes) [67, 68]. Data from Manya 6 well reveals that salt deposits are primarily found in lower intervals of the Ouldburra formation. The salts are interbedded with calcareous siltstone and carbonate. In 1987, Dunster identified two shallow upwards sedimentary cycles, e.g., the halite siliciclastic cycle and halite mixed carbonate siliciclastic cycle. Both cycles are part of upper relief sandstone and lower Ouldburra formation [69]. The thickness of Cambrian sediment in Winkson 1 wellbore was 594 m [67]. Basal relief sandstone has a thickness from 573 to 695 m. This layer comprises multiple formations such as limestone, salt, siltstone, and sandstone. Moreover, Manya 6 well has a 350 m uniform and interbedded halite layer. In early 1980s, 2D seismic data provided the images of subsalt sequences and salt structures. These images give a better understanding of halokinetic evolution. Salt dome and related trap styles have been identified on seismic line N83-006 and Seismic line T82-055 as reported in a study by Simeonova and Apak. [70].

The officer basin contained the dome type salt structure. The maximum salt layer thickness was reported 350 to 695 m. These dimensions meet the standard design feature for the salt cavern creation. The faulted anticline structure may raise the security concern of cavern stability [68, 71-75]. The officer basin comprises interbedded halite rock, limestone, siltstone, sandstone and other salts. However, limestone may react with H_2 and thus trigger hydrogen conversion and contamination through redox reactions [76-79]. Moreover, brine water of wells drilled in the Officer basins gives high concentration of SO_4^{2-}, which likely evolves sulphate reducing bacteria microbial activity [80].

The non-uniform diapirs are identified in the basin. Different formations beds, including halite, carbonate, anhydrite, and sandstone were in the diapirs. Previously, these diapirs received significant attention due to their possible hydrocarbon trap style [70, 81]. Moreover, anhydrite, carbonate and presence of some of Ca^{2+} and SO_4^{2-} in the brine of the drilled wells may trigger microbial activity leading to release of H_2S during hydrogen storage [67].

2.1.3 Advalae Basin

Boree salt deposits are widely found in the Advalae Basin, Queensland [82, 83]. Drilling data provided geological information about the basin. However, the area lacks exploration data in general [84]. Investigators observed that Boree salt formations are deposits of the Palaeozoic era and Devonian period [84]. Marine conditions emerged due to the thrusting with the Warrego fault forming the deposition of salt in the bedded structure. Boree salt deposits are >90% halite formation [85]. The thickness of Boree salt is 500 m. It is spread for over 100 km next to the present creek arch. The halite formation has some minor traces of mudstones and anhydrite along with inter-bedded sylvite minerals (potassium). Overlying sedimentary rock emerged in the system due to reactivation of basement faulting. Thus, these salt domes like salt pillows are sealing rock for petroleum reservoir and show potential salt deposits in the basin. The proper analysis of wellbore drilled formations, coring and exploration survey data will be required to construct the caverns in the basin. Figure 3 illustrates the presence of halite deposits in the Advalae Basin.

2.1.4 Canning Basin

Canning basins cover onshore and offshore areas of 400,000 km^2 and 165,000 km^2, respectively. Mallowa and Minjoo salts are recognised largest halite deposits. These salts are expanded in an onshore area of 200,000 km^2 in the WA [86, 87]. The average size of salt deposits was 800 m thick at a shallow depth of 1000 to 2000 m in Canning [86, 87]. This study selected the study area of Willara Sub-basin in Canning. Figure 3 shows study area and presence of halite deposits in the Canning. Table 1 lists well names, basins, stratigraphy, and halite thickness.

Table 1 details drilled wellbores containing halite salt thick units in the canning basin.

Geological period	**Well name**	**Source WAPIMS* [88]**	**Basin**	**Formation covers zone of interest**	**Top of salt horizon (m)**	**Salt thickness (m)**
Llandovery	Fruitcake 1	XRD data	Canning (Broome platform)	Mallowa salt	638	470
NA	Frome Rocks 1	Composite well log	Canning (Jurgurra Terrace)	Mallowa salt	687 m	594 m
NA	Nangu 1	Formation evaluation log	Canning (Willara Sub basin)	NA	NA	NA
NA	Carina 1	composite log	Canning (Broome platform)	Carribuddy	926	**306**
NA	Wood Hills 1	Composite log	Canning	NA	NA	NA
Llandovery	Sally May 1	Composite log	Canning	Mallowa salt	1311 m	72 m
Silurian	Willara 1	Composite log	Canning	Carribuddy	1280 m	480
NA	Willara Hill 1		Canning	NA	NA	NA
Silurian Devonian	Vela 1	WAPIMS*	Canning	Carribuddy group units A, B	965 m	625 m
NA	Gingerah Hill 1	Composite log	Canning	Carribuddy units A, B	963 m	502 m
NA	Musca 1	Composite log	Canning	Carribuddy	1041 m	180 m
Llandovery, Upper Ordovician	Looma 1	Composite log	Canning	Mallowa	584	533 m
				Minjoo	1163	29 m

Early Palaeozoic	Brooke 1	Drilling report	Canning	Carribuddy unit B	977 m	735
				Unit C halite/shale	1712 m	323 m
Silurian to lower devonian	Pegasus 1	Composite log	Canning	Carribuddy	1400 m	650 m
Pre-Permian	Willara 1	Composite log	Canning	Carribuddy	1280 m	183 m
NA	Munda 1	Composite log	Canning	Salt not found.	NA	NA
NA	Munro 1	Composite log	Canning	Salt not found.	NA	NA

*WAPIMS stands for Western Australian Petroleum and Geothermal Information Management System.

The coastal area and the proposed salt structures are within 50 to 60 km. The location is important in terms of trade and geolocation. The distance was measured using Geoview, WA tool [89]. Table 2 summarises the geo-constraints or surface limitations that were included in selecting the appropriate area for the development of the caverns in Canning. We have applied all possible constraints and selected eligible area for the placements of salt caverns. Moreover, the average distance of the proposed study area in Willara Sub-basin, Canning is around 63 to 100 km away. Water supply infrastructure will deliver seawater from seashore to construct salt caverns. Similarly, Ennis-King KM and Strand [90] documented a report for geological hydrogen storage and mapped out the options in Australia. Several factors were discussed in the report including the effect of the capital cost of brine pipelines and lagoons for construction of salt cavern.

Table 2 Constraints used in the land eligibility for the construction of salt caverns in Canning Basin

Special category lands	Availability
Geo-heritage site	NA
Section 57 (2AA) Australian Mining Act	NA
Conversations estate	• Kurriji Pa • Yajula Nature reserve • Karlamilyi National Park
Section 9 for precious metals	NA
Property of the Crown	NA
Natural condition above the surface	NA
Kimberly National Heritage Area	NA
Biodiversity areas	NA
Towns	NA
Aboriginal Heritage places	NA
Special agreement settlement	NA
WA coast	H_2 generation site would be 63 km to 70 km from the salt deposits.
Roads	The salt deposits are ~49-55 km from Great Northern Highway.
Land use planning	NA

Mallowa salt Canning contains a thick unit of halite salt as illustrated in the correlation diagram Figure S2 [47]. Moreover, bromide concentration increases from 60 to 270 ppm with depth. Halite layer thickness and composition indicate that Canning basin has potential for the construction of an underground salt cavern for hydrogen storage (Table 3). The relationship between the geological time, salt basins and selected salt deposits are illustrated in Figure 4.

Table 3 Comparison of Australian salt basins, average salt thickness, and salt structure in the different states for construction of salt caverns for hydrogen storage

Geological basin	Geological description	State	Average Thickness (m)	Structure	Ref
Mallowa Salt, Canning	• Inter-bedded halite • Red/green mudstone • Anhydrite and dolomite	Western Australia	• 695 m min • 800 m max	• 532 m thick salt diapir. • Inter-bedded halite rock	[49, 86, 91]
Minjoo Salt, Canning	• Orange, red-brown, clear to translucent halite inter-bedded • Reddish-brown partly dolomitic claystone.	Western Australia	• 40 m min • 313 m max	• Formation beds	[46, 49, 92]
Amadeus salt	• 115000 km^3 volume of Gillen evaporite • Halite deposits are present in the north-central and eastern basin areas.	Northern Territory, Western Australia	• 810 m min • 2100 m below GBI*	• Formation, beds, salt anticline, salt domes.	[46, 63, 93]
Advalae salt	• Amongst largest salt deposit in the world. • Largest potash and halite salt deposits. • Expanded in ~640 km^2 area.	Queensland	• ~500 m	• Large deposit of halite (90%) and some portion of salt has a dome structure.	[94]
Officer salt	• The Eastern Officer basin has a lower Cambrian salt deposit. • Considerable salt in thick sections of Browne formation	South Australia, Western Australia	• 350-695 m	• Inter-bedded salt • Salt diapir in central western officer basin.	[67, 68]

*GBI stands for Gosses bluff impact.

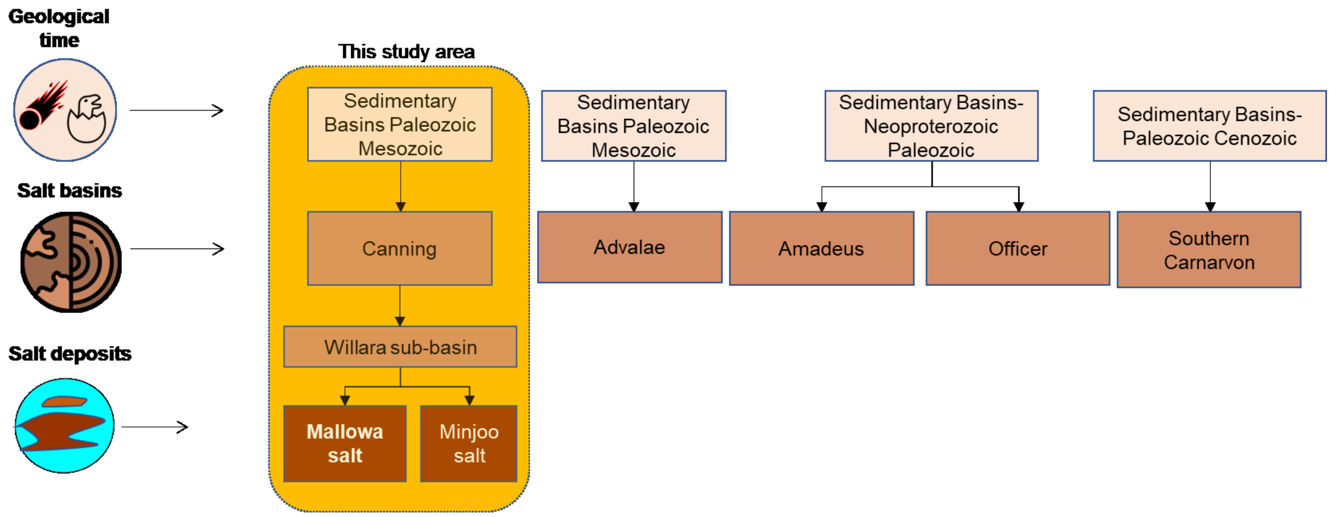

Figure 4 highlights the relationship between the geological time, salt basins and proposed salt deposits. This Figure shows that the Canning basin (our study area) is from the sedimentary basin Paleozoic (542 million to 251 million years ago) and Mesozoic (251 million to 65.5 million years ago) geological time scale.

3 Methodology

A preliminary overview of salt deposits was identified using the Australia Hydrogen opportunity tool (AusH_2), Geosciences Australia [66] to quantify Australia's onshore salt deposits and their potential for hydrogen energy storage. The detail of the AusH_2 tool information is provided in the supplementary information. Relevant geology and salt structure information were identified, e.g., bedded and salt dome using literature work [85, 92]. The Geosciences Department, the government of Australia provides halite deposit data shape files. These data files were used to draw an adequate salt map in different basins [66]. Then, a concise assessment of salt basins was conducted based on drilling, coring, wellbore logs, and exploration data. The methodology of this study is provided in Figure 5.

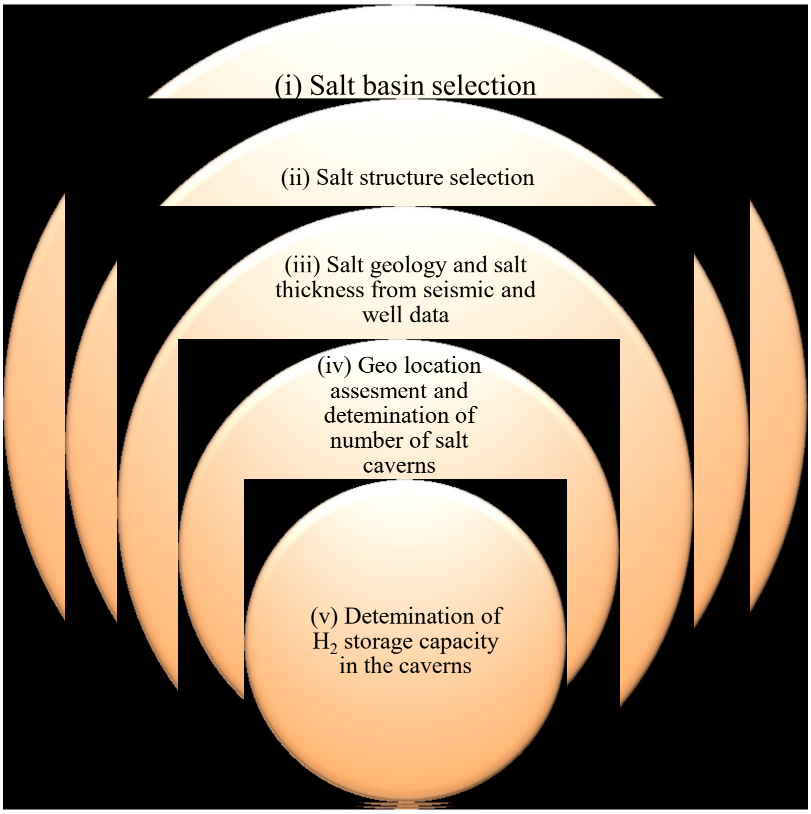

Figure 5 Flow chart of the methodology

3.1 Geo Location Assessment

The Geoview tool system (GTS) was used to evaluate the potential location for the construction of salt caverns [89]. Underground salt caverns could also influence the area on the surface. Leakage during salt cavern construction may cause the earth's surface subsidence problems. Besides, salts have adequate thickness, tight permeability, and self-healing properties. These salts can trigger the problems of inappropriate cavern shape, stored fluid loss, damage cement layer and wellbore casing corrosion [95]. Importantly, loss of the cavern's roof and early cavern collapse may also occur. These damages can interrupt the gas injection/withdrawing operation [60].

3.2 Design Features and Operational Limitations of the Salt Caverns

The operational limitations for constructing salt caverns in the bedded rock salt system were taken from studies [60, 96, 97]. The minimum thickness of the salt cavern's hanging wall was maintained 75% of the salt cavern's diameter. Moreover, the footwall thickness is maintained at 20% of the cavern's diameter [97]. The salt layer must be 200 m thickness for the appropriate construction of the salt cavern and its safety in bedded salt [60]. Cavern volume was made constant 500000 m^3. Diameter and height were selected 84 m and 120 m, respectively. The separation distance between each cavern was maintained 4 times of the cavern's diameter in between caverns' walls [60, 96, 97]. The spacing value between the caverns in a bedded salt system was taken from the previous study which reported the construction of salt cavern for hydrogen storage [60]. A variety of techniques has been proposed for the calculation of distance between two salt caverns. Zhang *et al.* [71] conducted a numerical simulation. They predicted that cavern's pillar width with a pillar-to-diameter (P/D) ratio of 1.5 could meet the tightness standard for strategic petroleum and natural gas storage in the salt cavern. Hence, the simulation results show that seepage velocity of natural gas is greater than crude oil in the interlayers of cavern. Consequently, the seepage area of natural gas salt caverns in comparison to crude oil salt caverns can be high. This seepage area starts to join together leading to an increase in the pore pressure in the middle of pillars after modelled time of 15 years [71].

Caglayan and her team [60] evaluated technical hydrogen storage potential across Europe in bedded salt deposits. The study suggested that total on- and offshore hydrogen energy storage potential is 84.8 PWh_{H_2} in Europe. The highest national hydrogen energy storage potential was determined in Germany which is 9.4 PWh_{H_2}

using development of salt caverns with a spacing of 4 times the cavern diameter. Certainly, the proposed spacing approach can result in high spacing between two caverns and impact the areal extent of salt deposits, consequently minimizing the number salt caverns in the region. Basically, density (ρ) and viscosity (μ) of hydrogen are very low when compared to methane and CO_2 as depicted in Table 4. Thus, low viscosity and low density of hydrogen can result in high seepage velocity and increase the risk of hydrogen leakage in the interlayers around the cavern. Hence, researchers recommended a high separation distance between hydrogen salt caverns when compared to salt caverns designed for CO_2, and methane storage [60, 96]. Therefore, we have selected spacing between each cavern i.e., 4 times the diameter of cavern in our work to avoid hydrogen seepage and leakage issues. The design features of proposed caverns are within the range and match typical parameters of salt caverns as presented in Table 5.

Table 4 Density and viscosity of different gases at proposed salt cavern storage conditions at 333.1 K and 20 MPa [98-103]

Gas	Density (kg/m^3)	Viscosity (cp)
H_2	13	0.009
CH_4	129	0.018
CO_2	723	0.06
N_2	188	0.023

Table 5 Features of a typical salt cavern for underground hydrogen storage

Parameter	Description	Refs
Formation	Halite	[104]
Salt layer thickness	>200 m	[41, 105, 106]
Salt structure	Dome, bedded	[105]
Cavern depth	~500 to 2000 m	[105, 106]
Cavern height	~120 m	[105, 107]
Cavern volume	500000 m^3	[41, 80]
Operating pressure	20 MPa	[105, 106]

3.3 Estimate Number of Salt Caverns and Energy Storage Capacity

We have used the following steps and determined the number of salt caverns using rectangular and triangular patterns in Mallowa salt deposits in Willara Sub-basin, Canning. A rectangular pattern is number of circles (i.e., salt caverns) with rectangular placement in a rectangle. Additionally, triangular pattern is number of circles with triangular placement in a rectangle.

a. Minimum thickness

Figure 6 shows isopach map for Mallowa salt deposits in Willara Sub-basin, Canning basin.

Minimum salt thickness required= cavern height + foot wall thickness + hanging wall thickness (1)

= (120 + 8.4 + 63) m = 191.4 m

A minimum of 191.4 m thick salt is needed for constructing the salt cavern. We examined the proposed area in Mallowa salt with salt layer thickness greater or equal to 200 m (Figure 6c), which is in line with the previous publication [47].

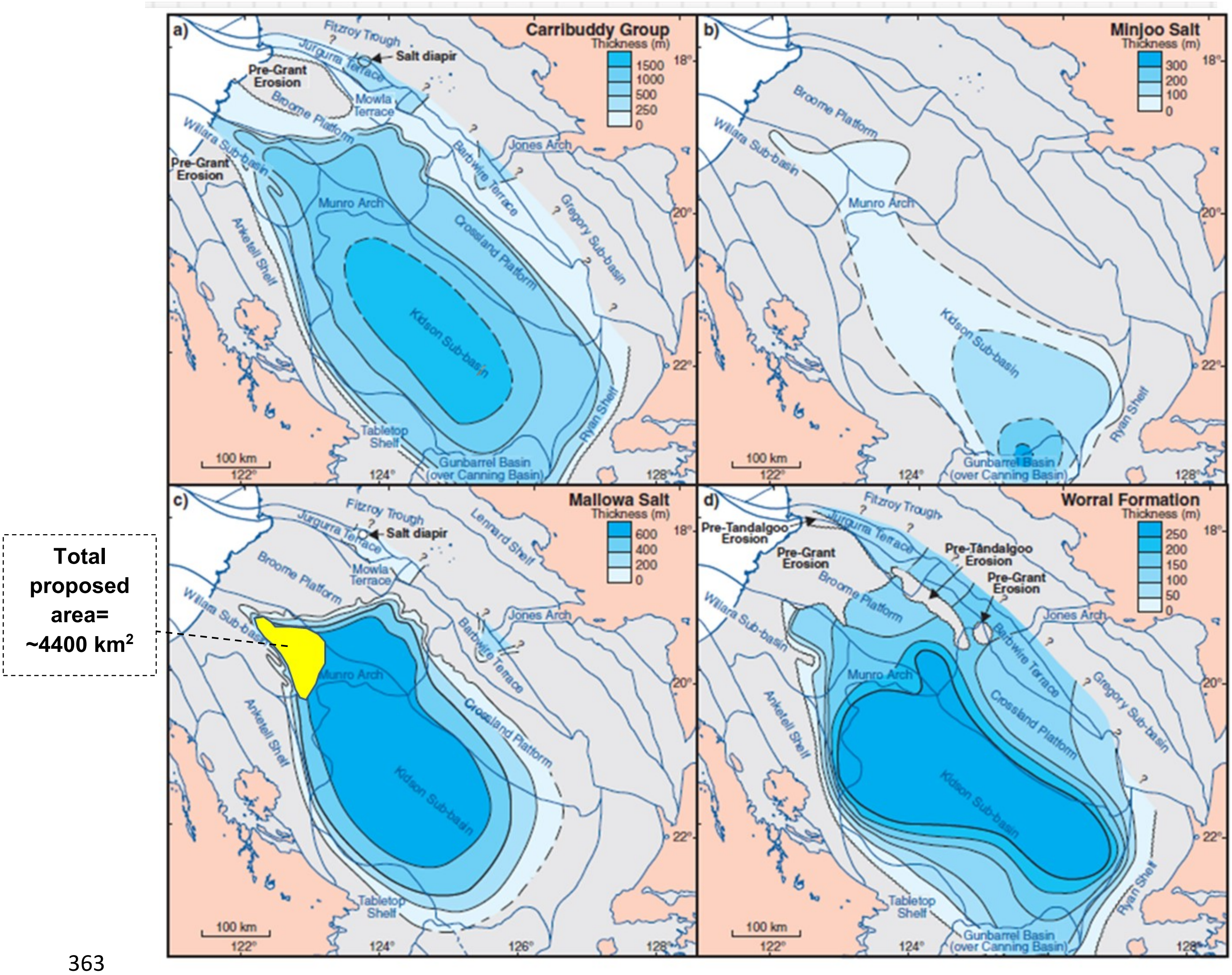

Figure 6 Isopach maps illustrate salt deposits: (a) Carribuddy group salts (b) Minjoo salt (c) Mallowa salt (d) Worral formation. Modified after [47]

b. Selection of proposed area

Referring to Figure 6c, we determine the total area for salt caverns construction in Willara Sub-basin at 100 km scale = 4500 km^2

c. Safe distance in between each salt cavern

The safe distance between two salt caverns is 4 times the diameter of the cavern [60] as illustrated in Figure 7a.

Safe distance in between two caverns= 4× Diameter of salt cavern (2)

= (4 × 84) m = 336 m.

Thus, *total safe salt cavern domain area diameter= Salt cavern diameter+ Safe distance* (3)

= (84+336) m = 420 m

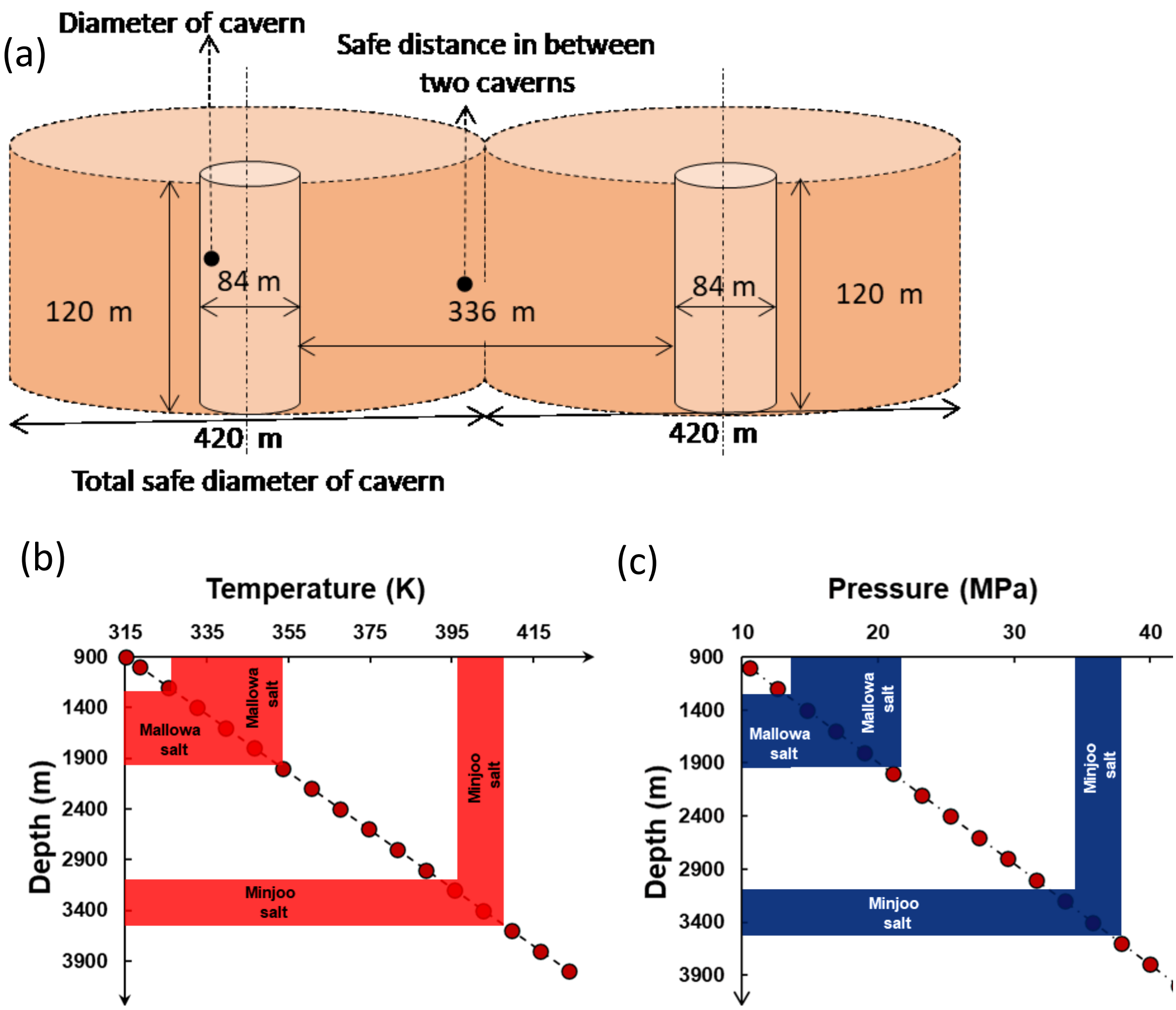

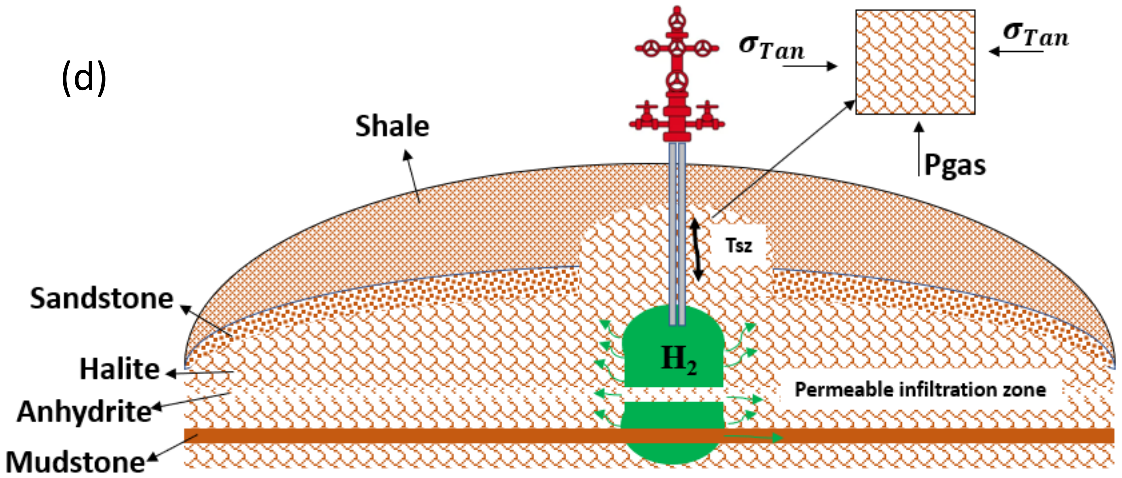

Figure 7 (a) Dimensions of salt cavern including safe distance in between two caverns, diameter of the cavern, height of the cavern and the cavern's safe domain area (b) Temperature profile (c) Pressure profile of Mallowa and Minjoo salts (d) Schematic of gas seepage in interlayers around salt cavern and design parameters.

d. Safe area of cavern

Area of each cavern= $\pi(r)^2$ (4)

$= 3.14\ (210\ \text{m})^2 = 138{,}474\ \text{m}^2$

e. Number of salt caverns with rectangular patterns in a rectangular area

Online software [108] was used to estimate the maximum number of salt caverns that fit into proposed rectangular area.

Area of rectangle= $l \times w$ (5)

$= 67000\ \text{m} \times 65800\ \text{m} = 4.39 \times 10^9\ \text{m}^2$

Input parameters are the proposed rectangular area length= 67000 m. The proposed rectangular area width= 65800 m. Hence, we found that, the area of each salt cavern=5542 m^2 and total area of all caverns=135717934 m^2. Moreover, maximum number of the caverns with rectangle pattern inside the rectangular area= 24490.

f. Number of salt caverns with triangular pattern in a rectangular area

The same online software [108] was used to estimate the maximum number of salt caverns that fits into proposed rectangular area were calculated using same online program [108]. The total proposed rectangular area is 4.3943× 10^9 m^2. Moreover, input parameters are the proposed rectangular area length= 67000 m, the proposed rectangular area width= 65800 m, a diameter of each salt cavern=84 m and safe distance between each salt caverns = 336 m. Hence, we found that, area of each salt cavern =5542 m^2, total area of all caverns= 156732323 m^2, and a maximum number of caverns= 28282. Hence, it shows that number of the caverns with triangular patterns is greater than rectangular pattern in the same rectangular area. Therefore, total area is higher for the salt caverns placed with triangular pattern when compared to rectangular pattern in the area.

3.4 Determine Hydrogen Energy Storage Capacity in Salt Caverns

The estimation of salt caverns hydrogen storage capacity at specified reservoir conditions to develop the field scale storage plan [17, 109]. The energy storage capacity of each salt cavern was determined using Equation 6 [60, 110] at typical salt cavern depth conditions of 333.15 K and 20 MPa. These conditions meet existing Mallowa salt deposit pressure and temperature conditions.

$$E_{H_{2T,P}} = \rho_{H_2} \times MW_{H_2} \times V_{salt\ cavern} \times HHV_{H_2} \qquad (6)$$

$E_{H_2 T,P}$ = hydrogen energy storage capacity at 333.15 K and 20 MPa according to depth settings of caverns, ρ_{H2} = density of hydrogen at 333.15 K and 20 MPa, $V_{salt\ cavern}$ = volumetric capacity of salt cavern, MW_{H2} = molecular weight of hydrogen, and HHV_{H_2} = higher heating value of H_2.

3.5 Determine Safe Working Gas Capacity in Salt Caverns

Maximum and minimum hydrogen gas pressures in salt caverns must be controlled and constrained to 80% (maximum) and 24% (minimum) of overburden pressure [60]. Safe gas pressure can be calculated using equation 7.

$$\text{Safe working gas capacity} = (P_{max} - P_{min}) \times E_{H_2 T,P} \qquad (7)$$

$E_{H_2 T,P}$ = hydrogen energy storage capacity at 333.15 K and 20 MPa, P_{max}=maximum operating pressure, and P_{min}= minimum operating pressure.

3.6 Calculate Admissible Hydrogen Gas Pressure

Researchers investigated that admissible hydrogen injection pressure of fluid should not be greater than 80% of overlying formation pressure or formation fracture breakdown pressure at casing shoe depth [111]. Some investigators believe that maximum admissible gas pressure could be 80% of overlying formation pressure [112, 113]. Figure 7 (b and c) illustrates that Mallowa salt is safe and meets the operating condition of salt cavern geo-storage at 900 to 1900 m depth, as previously reported for some caverns in Germany [105]. Similarly, admissible gas pressure could be proposed 20 MPa for the caverns in Canning. The injected gas pressure is less than 80% of the overlying formation pressure [112-114].

However, an increase in separation distance between two caverns can minimize the gas infiltration failure. To ensure gas infiltration free salt cavern zone system, tangential rock stress and gas pressure must meet desired safety factor (S_f). Thus, cavern tightness can be achieved after non-infiltration zone has an adequate thickness (Tsz) in the design (Figure 7d). Therefore, Equation 8 must be satisfied to mitigate gas infiltration in the safe zone [113].

$$\sigma_{Tan} \geq S_f P_{gas} \quad (8)$$

σ_{Tan} = Tangential rock stress (MPa), Sf= desired safety factor, and P_{gas} = gas pressure (MPa). The relationship between in-situ stress and maximum gas pressure is given in Equation 9 [113],

$$S_f = \frac{\sigma_{min}}{P_{max}} \quad (9)$$

σ_{min} = minimum in-situ stress, and P_{max}=maximum gas pressure (MPa)

4 Result and discussion

4.1 Potential of Salt Cavern Construction in Canning

Table 6 provides the benchmark selection of different salt basins for the construction of underground hydrogen storage salt caverns. The proposed benchmark shows that the Canning basin is most promising option for the construction of the caverns because this basin is rich in seismic, drilling and salt deposits data. Canning mostly contains halite and anhydrite with anomalous values for K_2O and Br at a different isopach map lines interval of 250 m, 500 m and 750 m (Figure 8a). Gingerah Hill1, Brooke 1, and Vela 1 and other wells reportedly show the presence of halite thick units in the basin (Figure 8b). The presence of the Admiral Bay Fault Zone between Vela 1 and Musca 1 can be a concern for the construction of salt caverns in the region. These faults can leak the gas and connect two caverns [115, 116]. Thus, salt caverns must be placed at a safe distance from the fault. The safe distance from fault line must be greater than 2.5 times the salt cavern's diameter as reported in the study [117].

(a)

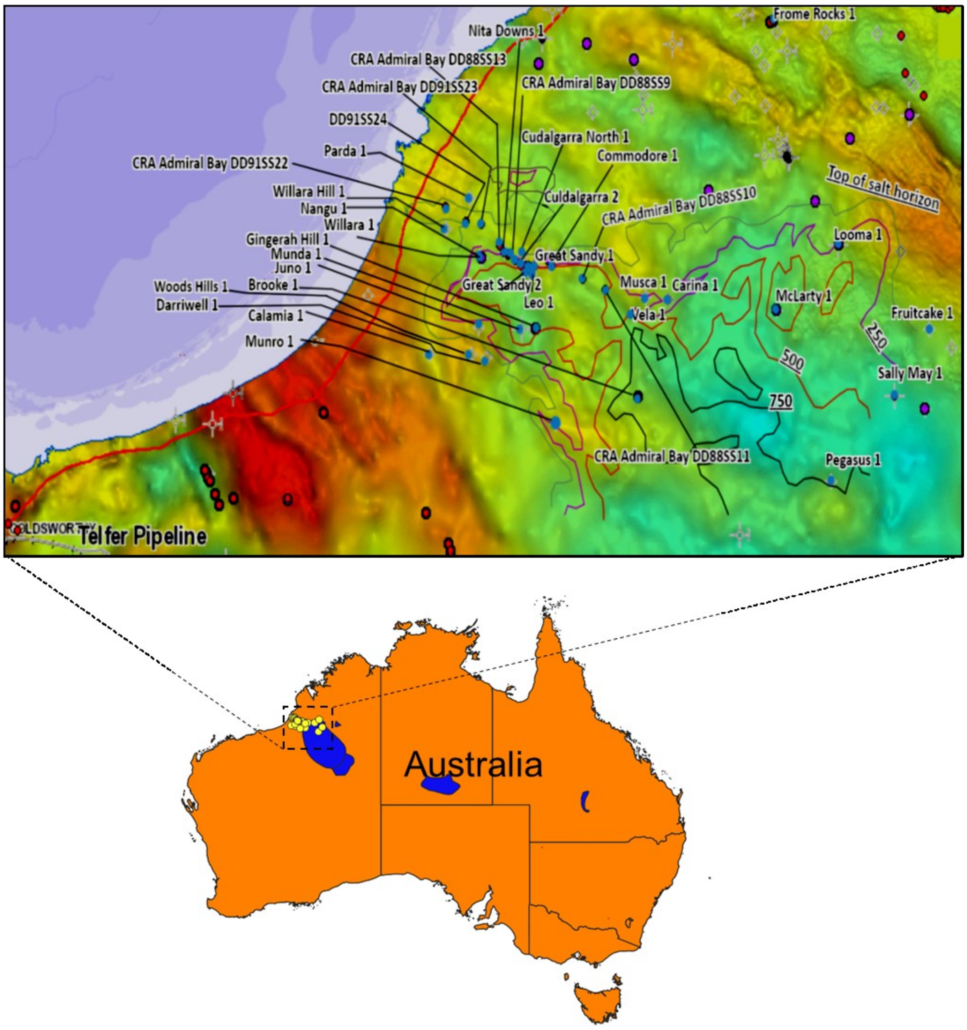

(b)

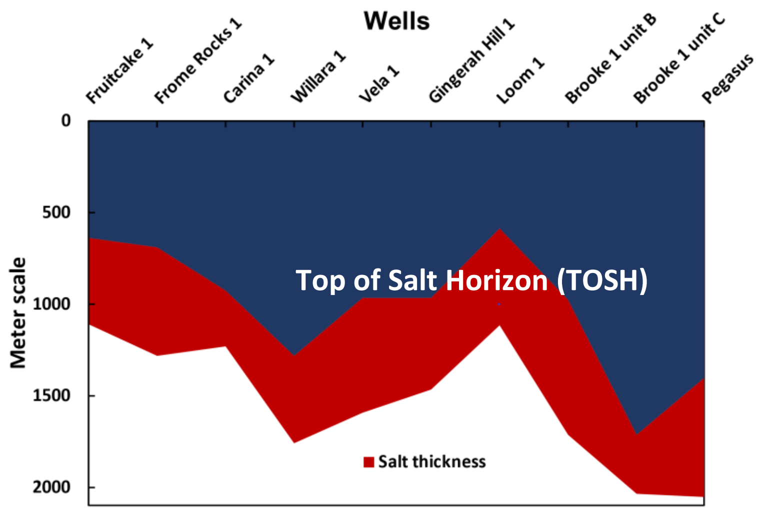

Figure 8 (a) The gravity map and the information of the wells located in the Canning (b) salt thickness and top of salt horizon information are provided for each well located in the Canning

Table 6 Proposed benchmark for the selection of Australian salt for underground hydrogen storage

Salt basins	Advalae	Canning	Amadeus	Officer
Realistic experience	Insufficient	Insufficient	Insufficient	Insufficient
Seismic data	Low	Fair	Fair	Low
Petroleum well data	Fair	Fair	Fair	Fair
Halite	Excellent	Fair	Fair	Fair
Interbedded Halite and Anhydrite	Low	Fair	NA	Fair
Anhydrite	Low	Fair	Excellent	Fair
Microorganism information	Insufficient	Insufficient	Insufficient	Insufficient
Salt structure	Dome	Bedded, Dome	Bedded, Dome	Dome, interbedded
Exploration cost	Fair	Low	Fair	Fair

Well Brooke 1 logging information, coring, and drilling data show that Mallowa salt consists of a large evaporate water body (saltern, pale brown colour) in Willara Sub-basin, Canning. The thickest unit of evaporate in the Carribuddy group is Mallowa salt.

Table 7 shows the presence of Mallowa salt and sequence of formations from top to bottom for the Carribuddy group. However, it is thin across the northward Broome platform and forms a patchy subcrop. Equivalent halite salt transformed into salt structures [118] as shown in the supplementary information Figure S3. Further, Mallowa salt is overlain by mottled mudstone (extensive unit) and anhydrite [86]. The consistent presence of Na_2O and total salt percentage were observed in the samples. These are two kinds of samples, i.e., separated=separated minerals and whole=all minerals recovered at depths from 750 to 2150 m. These indicate a rich salt deposits environment. The geochemical data suggested the presence of Bromine 90 to 670 ppm in separated and more than 150 ppm in whole samples of halite (95 wt%) as illustrated in Figure 9 (a and b). Bromine concentration can catalyse mining solution process but may trigger precipitation of potash evaporates issues.

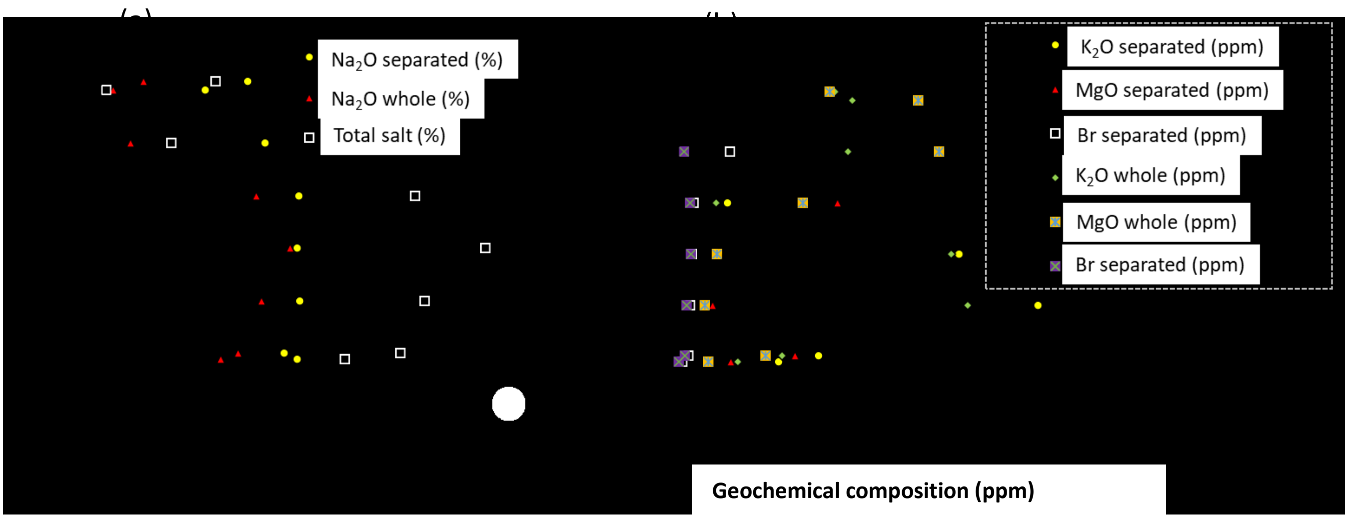

Figure 9 Geochemical composition of Brooke 1 well formation water (a) Percent of salt present in the formation water (b) presence of MgO, potassium oxide and Bromine in the formation water.

Table 7 The sequence of formation layers from top to bottom for Carribuddy group, Canning

Formation (From top)	Characteristics
Sahara formation	• Dolomite • Siltstone
Mallowa salt	• Halite • Minor anhydrite • Mudstone • Dolomite
Nibil formation	• Mudstone • Dolomite • Siltstone
Minjoo salt	• Halite • Mud stone • Dolomite
Borgabinni formation	• Mudstone • Dolomite

Between 1960 to 2000, a seismic survey was carried out from time to time to explore the Willara Sub-basin. The seismic image for the basin is provided in Figure S3 in the supplementary information. Further, well intersection data and seismic data confirm that Mallowa salt exists in the Willara Sub-basin. Mallowa salts have maximum thickness of 950 m in the south of Munro Arch [119, 120]. The Minjoo salt has mostly emerged in the south-eastern part of Willara Sub-basin. Seismic information reveals that Minjoo has a 100 m salt thickness near the East margin of the Willara Sub-basin [119]. The continuity and presence of the salt between Vera 1 and Willara 1 need to be clarified because of imaging limitations and lack of seis mic data [49, 119].

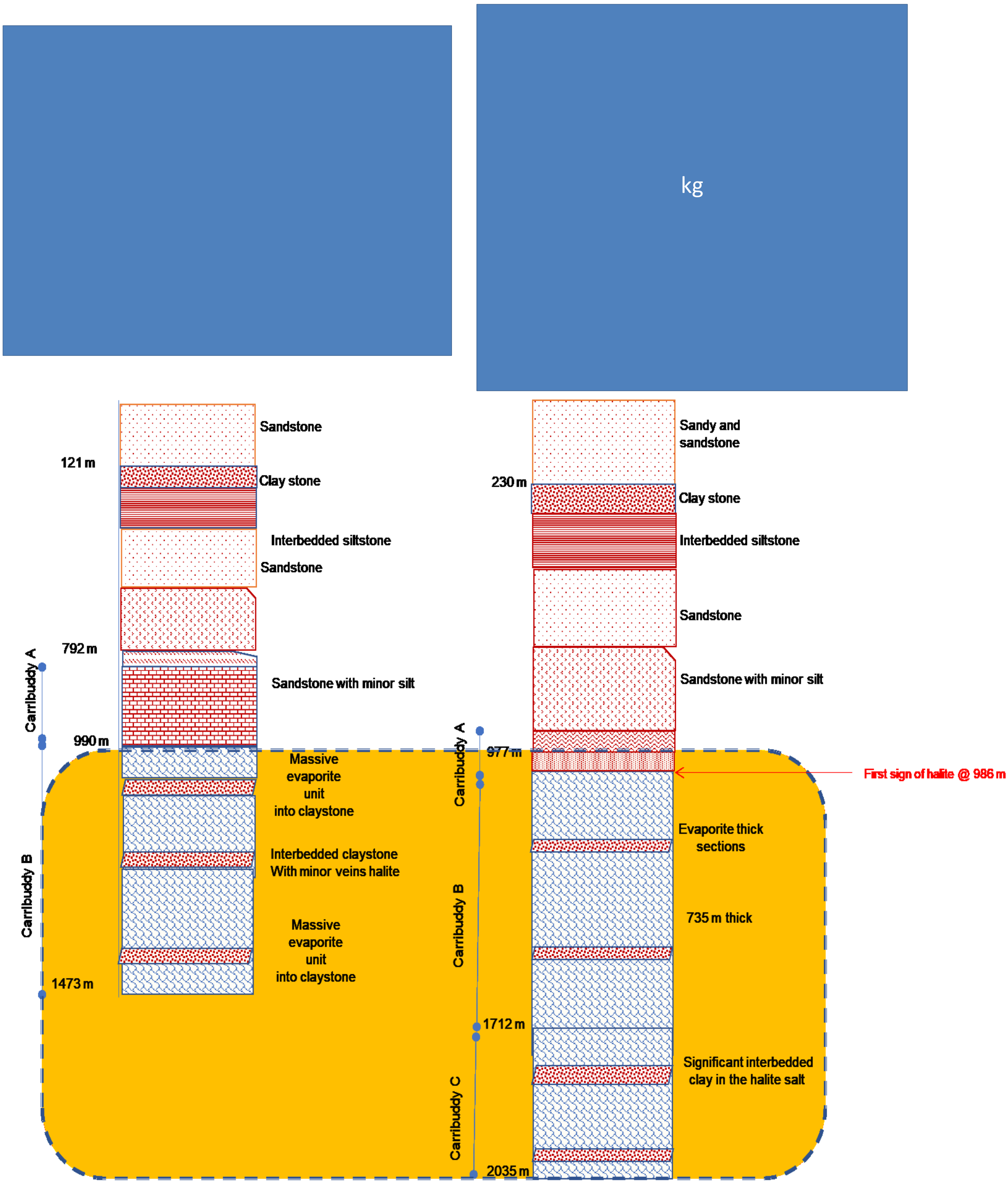

Figure 10 Well logging, drilling cutting, and coring of Gingerah hill 1 and Brooke 1 were collected and correlated. Both wells contain interbedded sheaths of thick to thin clay in thick halite interval.

In 1987, Brooke 1 exploratory well was drilled in the Willara Sub-basin, Canning basin to a depth of 2035 m as illustrated in Figure 10. The well drilling program was designed to drill and explore the thickness of Carribuddy unit B rock salt. Drilling bit intersected 735 m thick rock salt layer in Carribuddy unit B. The first sign of salt rock was identified at a depth of 986 m. Coring was carried out from 863 m to 2035 m. Figure 11 (a and a') shows the images of cores from Brooke 1 well drilled in the Canning basin.

In 1986, Gingerah Hill 1 was spudded at a total depth of 1473.5 m as depicted in Figure 10. Carribuddy A group started from 792 m. This group is composed of grey marl shale, a significant amount of claystone with red and green mottling, red and greenish mottled clay stone and veins of evaporitic mineral. Figure 10 summarises the formative assessment of Gingerah Hill 1 Carribuddy B group formation from 990 m to 1473 m. Figure 11 (b and b') illustrates images of cores from Gingerah Hill 1. The process of coring started from 506 m to 1430.1 m. Grey shale, grey mudstone, pebble sandstone and clay sand is common from 506 m to 729 m. Probably anhydrite was identified at 955 m along with grey and red mottled sandy claystone. The first sign of halite was observed as veins in the mottled claystone and scattered crystals at 963 m. The first predominate halite beds with 30 m thickness along with clay interbeds were located at the depth from 977 m to 979 m. The consistent presence of halite was observed along with above the formations until 990 m. In the Carribuddy B group, halite salt unit is located at 990 m depth where the rock salt exists as main lithology of the core. Two major lithologies were located namely massive and granular halite salts. Massive type rock salt is composed of interlocking halite grains which are in light brown to dark colour in the presence of clay as a minor constituent. Granular halite salt is readily discernible due to the large presence of interstitial clay and drilling activity. Gingerah Hill 1 drilling report provided adequate information about underground formations. For example, Type 1 and Type II halite rock cycles are comprised of randomly oriented interlock halite salt crystals due to the phase of early diagenesis. Both cycles were characterized by a small presence of anhydrite [87]. Overall, we demonstrate that thick evaporite sequence in the region could be an appropriate choice for the construction of an underground salt cavern to store hydrogen gas.

Brooke 1 well cores

Gingerah Hill 1 well cores

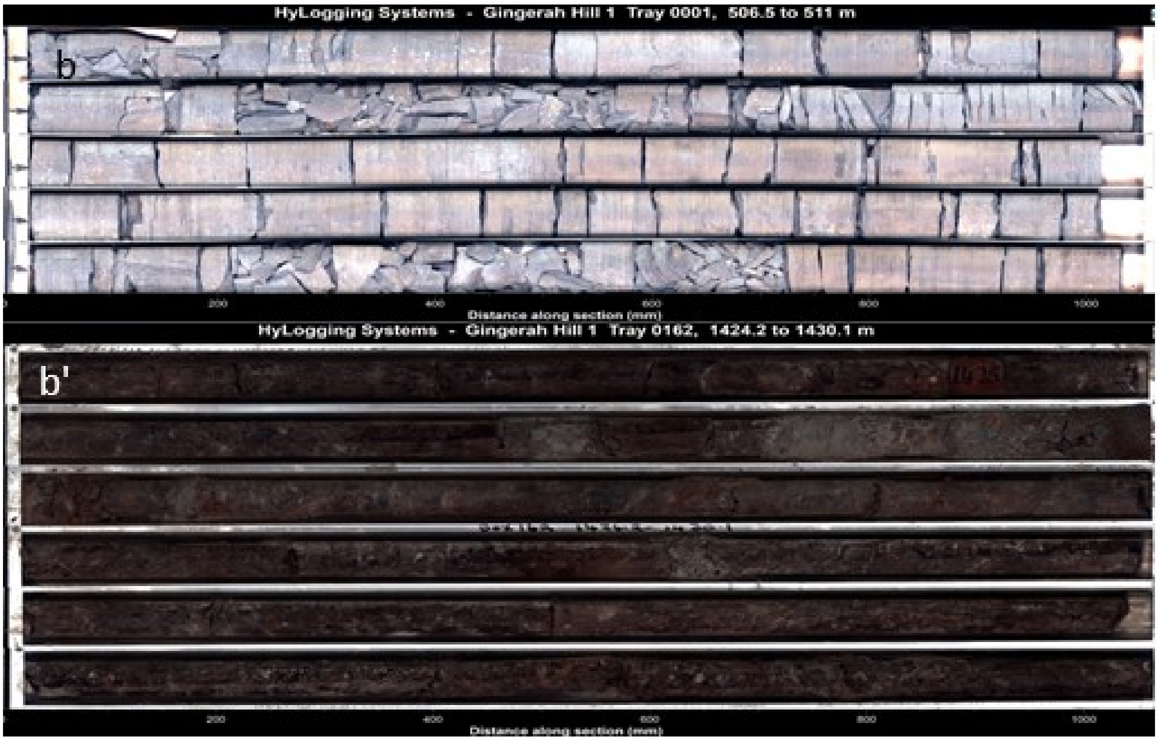

Figure 11 (a and a') Core sample of Brooke 1 well: 863 to 866 m core consists of grey silty shale, anhydrite, minor while, calcareous siltstone, and quartz grains. 866 m to 868 m: shale, dark green, minor pale grey shale, silty to sandy. 1505 m to 1510 m: Mainly rock salt with significant to minor clay (b and b') Core sample of Gingerah Hill: 506 to 511 m: Mostly grey shaly with thin sandy partings. 1424 to 1430 m: Coarsely crystalline rock in light brown colour, granular salt rock, clay patches, coarsely crystalline halite in light brown colour. Core images are taken from the Geoview tool online database, WA tool link is provided in the supplementary information.

4.2 Hydrogen Energy Storage Capacity in Canning

The evaluation of hydrogen energy storage capacity is key for implementing of underground hydrogen storage at a commercial scale. In our study, we have shown that Canning Basin is rich in bedded salt systems. Thus, we calculated energy storage capacity, i.e., 500000 m^3 capacity in bedded salt deposits as illustrated in Figure 12. This Figure shows that energy storage capacity of salt cavern increases with pressure and decreases with temperature. Energy storage data as illustrated in Figure 12 well matched with previous reference works [80, 110]. Figure 13 illustrates the hydrogen storage potential in Canning, Australia. Australia total energy consumption is 6196 PJ/year, according to the Australian Energy Update report published in 2020 [121]. We calculated total underground salt cavern energy storage capacity in the Mallowa salt of Willara Sub-basin. We estimated that 28282 salt caverns could store 14697.3 PJ/year of hydrogen energy which is more than enough to supply the energy demand of Australia and fulfill 57.8 % of hydrogen export demand as depicted in Figure 13. These energy storage estimates are based on the fixed volumetric capacities of each salt cavern of 500000 m^3 (bedded system). Hydrogen withdrawing efficiency and underground loss could influence the estimates and require further investigations. Table 8 provides estimated number of salt caverns and their hydrogen energy storage capacity. Figure 14 (a and b) illustrates that the number of salt caverns is determined in the rectangular area via rectangular and triangular patterns.

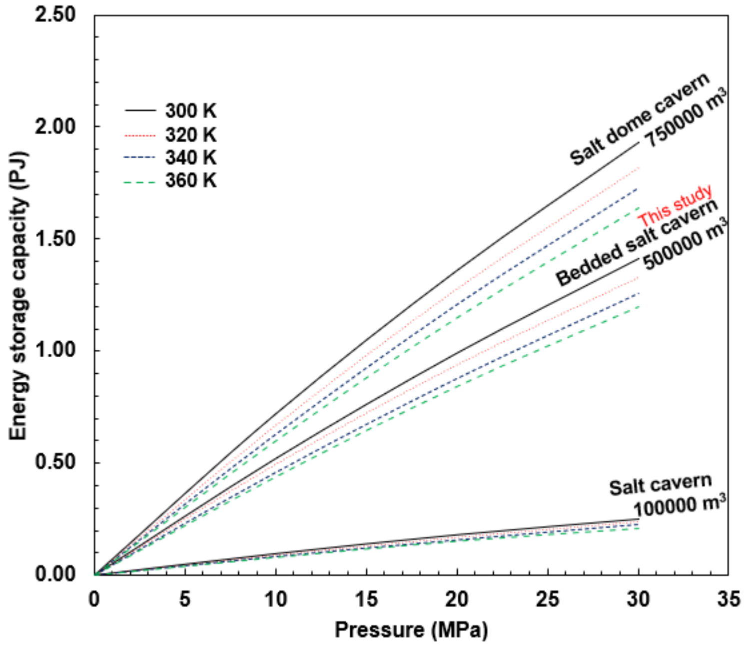

Figure 12 Energy storage capacity of a salt cavern with different sizes at variable geological conditions including pressure and temperature.

Australia contains other potential salt sedimentary basins i.e., Officer, Amadeus, and Advalae. However, they are far from port, hydrogen generation sites, and gas processing infrastructure. Thus, the most potential location is the Northwest area of the Canning Basin which is close to the Great Northern Highway, Telfer pipelines, Northwest Shelf gas facility and Pacific Hydro Australia Developments Pty Ltd hydrogen generation facility, i.e., in development. Therefore, we focus on the Willara Sub-basin, a part of Canning for creation of salt caverns. We present an approach for assessing the suitability of the salt deposits for hydrogen storage in the region.

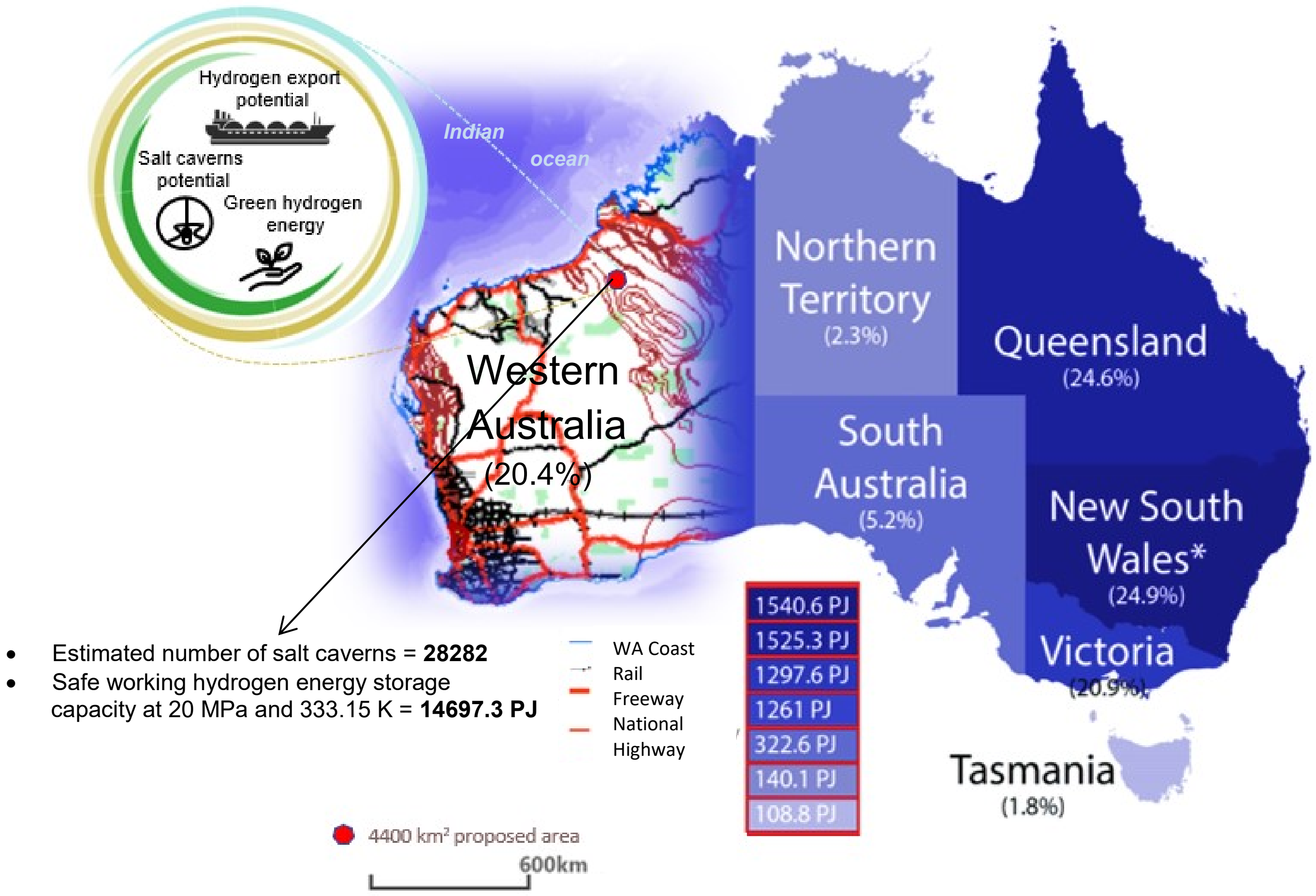

Figure 13 Map shows that Western Australia has immense potential to generate, export and store clean hydrogen through electrolysis of seawater, shipping hydrogen tanks and underground salt caverns. Further, the figure illustrates that the highest percent of energy is consumed by New South Wales which is 24.9% followed by Queensland (24.6%), Victoria (20.9%) and Western Australia (20.4%). The proposed number of salt caverns has the potential to store 14697.3 PJ of hydrogen energy in Willara Sub-basin, Canning Basin.

Table 8 presents number of salt caverns and hydrogen energy storage capacities in Western Australia

Salt basin	State	Depth and thickness	Pattern	Number of salt cavern	Total hydrogen storage capacity (PJ)	Total safe working hydrogen storage capacity (PJ)
Willara Sub-basin, Canning	Western Australia	~985-2035 m Depth 700 m thickness	Triangular	28282	26245	14697
			Rectangular	24490	22726	12726

*Energy storage capacity was measured at operating parameters of 333.15 K and 20 MPa.

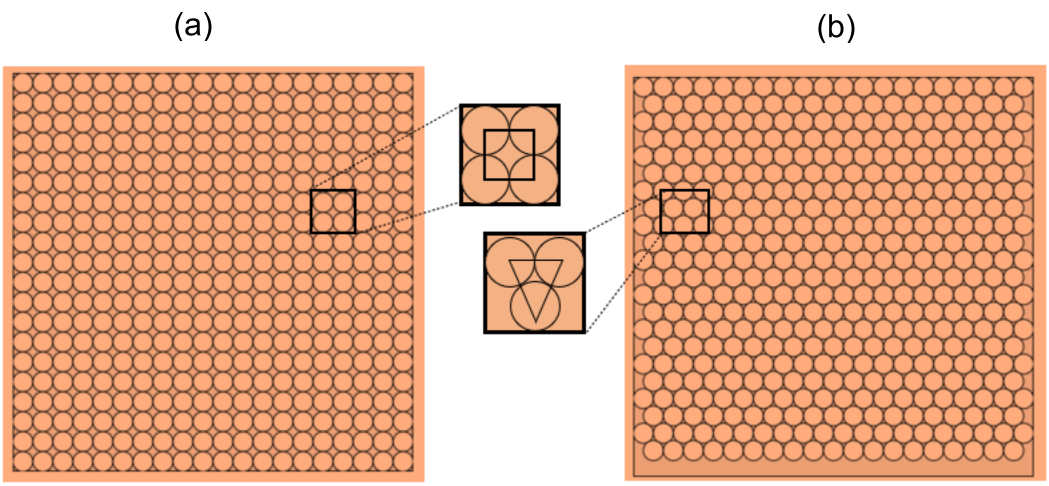

Figure 14 (a) Salt caverns are created in the rectangular area via rectangular placement of the caverns. (b) Salt caverns are developed in the rectangular area via triangular placement of the caverns

5 Conclusions

Underground hydrogen storage sites in Australia are identified. Hydrogen storage amount in these sites is estimated using geological data. The proposed study area has geo-economic importance because of its existence in the 100 km radius comprising of the Indian seashore, Telfer gas pipeline, and the Great Northern Highway. These benefits make the proposed area a potential storage and export facility for hydrogen in Australia. Additionally, the proposed area is free from geographical constraints for the salt cavern development. The seismic and isopach map data confirm the presence of Mallowa thick salt bed and their applicability for salt cavern construction. We estimated that ~28,282 salt caverns each 500000 m^3 can be constructed. These caverns are sufficient to achieve a full-development hydrogen value chain through cost-effective, large-scale, and safe storage of hydrogen energy for both domestic consumption and export.

6 Acknowledgment

The first author says thanks Government of Australia for awarding him Australian Government Prestigious RTP Ph.D. Scholarship T2 2021. We thank the geosciences Government of Australia for providing the necessary help and data associated with potential halite deposits.

7 Nomenclature

$AusH_2$	Australia hydrogen opportunity tool
Br	Bromine ion
Ca^{2+}	Calcium ion
$CaSO_4$	Calcium sulphate
CCS	Carbon capture and storage
COP26	Conference of the Parties 26th meeting
CO_2	Carbon dioxide gas
H_2	Hydrogen gas
$E_{H_2 T, P}$	Hydrogen energy storage capacity
EU	European Union
Ga	Giga annum
GBI	Gosses bluff Impact
GDO	Geological drilling order
GHGE	Greenhouse gas emissions
GTS	Geoview tool system
H_2	Hydrogen gas
H_2S	Hydrogen sulphide
K	Kelvin
l	Length
K_2O	Potassium oxide
km	kilometre
HHV_{H_2}	Higher heating value of hydrogen
m	Meter
MJ	Megajoule
MgO	Magnesium oxide
M_{H_2}	Mass of hydrogen
MPa	Megapascals
MW_{H_2}	Molecular weight of hydrogen
Na_2O	Sodium oxide
NT	Northern territory
P_{gas}	Gas pressure
P_{max}	Maximum gas pressure
P_{min}	Minimum gas pressure
PJ	Peta joule
ppm	Parts per million
QL	Queensland
r	radius
S	South
SA	South Australia
S_f	Design safety factor
SO_4^{2-}	Sulphate ion

$V_{salt\ cavern}$	Volumetric capacity of salt cavern
TOSH	Top of salt horizon
UHS	Underground hydrogen storage
w	Width
WA	Western Australia
WAPIMS	Western Australian Petroleum and Geothermal Information Management System
wt%	Weight percent
Y	Year
σ_{Tan}	Tangential rock stress
ρH_2	Hydrogen density

8 References

[1] M. Chaudry, L. Jayasuriya, S. Blainey, M. Lovric, J.W. Hall, T. Russell, N. Jenkins, J. Wu, The implications of ambitious decarbonisation of heat and road transport for Britain's net zero carbon energy systems, Applied Energy 305 (2022) 117905.

[2] X. Dong, J. Wu, Z. Xu, K. Liu, X. Guan, Optimal coordination of hydrogen-based integrated energy systems with combination of hydrogen and water storage, Applied Energy 308 (2022) 118274.

[3] IPCC, AR5 Climate Change 2014: Mitigation of Climate Change, 2014. https://www.ipcc.ch/report/ar5/wg3/. Assessed on 12th Feb 2022.

[4] UN, The Glasgow Climate Pact – Key Outcomes from COP26, 2022. https://unfccc.int/process-and-meetings/the-paris-agreement/the-glasgow-climate-pact-key-outcomes-from-cop26. Assessed on 12th Feb 2022.

[5] NASA, 2021 Continued Earth's Warming Trend, 2022. https://earthobservatory.nasa.gov/images/149321/2021-continued-earths-warming-trend#:~:text=Earth%20in%202021%20was%20about,popping%20up%20around%20the%20world.&text=The%20values%20represent%20surface%20temperatures,entire%20globe%20for%20the%20year. Assessed on 10th Jan 2022.

[6] NASA, Global Climate Change: Vital Signs of the Planet. https://climate.nasa.gov/. Assessed on 12th Feb 2022., 2022

[7] N. Times, Emissions Fell in 2009, Showing Impact Of Recession, 2011. https://www.nytimes.com/2011/02/17/science/earth/17emit.html. Assessed on 12th Feb 2022.

[8] J. Worland, How the Recession Accidentally Helped the Planet, 2015. https://time.com/3966553/recession-emissions-decline/. Assessed on 12th Feb 2022.

[9] A. Buis, A Degree of Concern: Why Global Temperatures Matter, 2022. https://climate.nasa.gov/news/2865/a-degree-of-concern-why-global-temperatures-matter/. Access on 30th Jan, 2022.

[10] N.P. Brad Plumer, Why Half a Degree of Global Warming Is a Big Deal, 2018. https://www.nytimes.com/interactive/2018/10/07/climate/ipcc-report-half-degree.html. Assessed on 29th August, 2021

[11] K. Mazloomi, C. Gomes, Hydrogen as an energy carrier: Prospects and challenges, Renewable and Sustainable Energy Reviews 16(5) (2012) 3024-3033.

[12] T.W.B. Group, CO2 emissions (Kt) 2022. https://data.worldbank.org/indicator/EN.ATM.CO2E.KT?end=2018&start=1960&view=chart. Assessed on 12th Feb 2022.

[13] T.W.B. Group, Global Population, 2022. https://data.worldbank.org/indicator/SP.POP.TOTL?start=2000. Assessed on 12th Feb 2022.

[14] EIA, Global Energy Review 2020. https://www.iea.org/reports/global-energy-review-2020/global-energy-and-co2-emissions-in-2020 Assessed on 23/01/2021. Assessed on 21 Jan 2023, 2020.

[15] S. van Renssen, The hydrogen solution?, Nature Climate Change 10(9) (2020) 799-801.

[16] J. Rosenow, R. Lowes, O. Broad, G. Hawker, J. Wu, M. Qadrdan, R. Gross, The Pathway to Net Zero Heating in the UK: A UKERC Policy Brief, (2020).

[17] A. Hassanpouryouzband, E. Joonaki, K. Edlmann, R.S. Haszeldine, Offshore Geological Storage of Hydrogen: Is This Our Best Option to Achieve Net-Zero?, ACS Energy Letters 6 (2021) 2181-2186.

[18] Y. He, Y. Zhou, Z. Wang, J. Liu, Z. Liu, G. Zhang, Quantification on fuel cell degradation and techno-economic analysis of a hydrogen-based grid-interactive residential energy sharing network with fuel-cell-powered vehicles, Applied Energy 303 (2021) 117444.

[19] J. Mouli-Castillo, N. Heinemann, K. Edlmann, Mapping geological hydrogen storage capacity and regional heating demands: An applied UK case study, Applied Energy 283 (2021) 116348.

[20] Q. Mugheri, T. Aneela, U. Aftab, M. IshaqAbro, S.R. Chaudhry, L. Amaral, Z.H. Ibupoto, Co3O4/NiO bifunctional electrocatalyst for water splitting, Electrochimica Acta 306 (2019) 9-17.

[21] G. Nascimento da Silva, P.R.R. Rochedo, A. Szklo, Renewable hydrogen production to deal with wind power surpluses and mitigate carbon dioxide emissions from oil refineries, Applied Energy 311 (2022) 118631.

[22] G. Australia, Hydrogen, 2021, http://www.ga.gov.au/scientific-topics/energy/resources/hydrogen Assessed on 19/04/2021.

[23] F. Sun, J. Qin, Z. Wang, M. Yu, X. Wu, X. Sun, J. Qiu, Energy-saving hydrogen production by chlorine-free hybrid seawater splitting coupling hydrazine degradation, Nature communications 12(1) (2021) 1-11.

[24] L. Zhang, Z. Wang, J. Qiu, Energy-Saving Hydrogen Production by Seawater Electrolysis Coupling Sulfion Degradation, Advanced Materials (2022) 2109321.
[25] M.F. Lagadec, A. Grimaud, Water electrolysers with closed and open electrochemical systems, Nature Materials 19(11) (2020) 1140-1150.
[26] T. Longden, F.J. Beck, F. Jotzo, R. Andrews, M. Prasad, 'Clean'hydrogen?–Comparing the emissions and costs of fossil fuel versus renewable electricity based hydrogen, Applied Energy 306B (2022) 118145.
[27] G. Brändle, M. Schönfisch, S. Schulte, Estimating long-term global supply costs for low-carbon hydrogen, Applied Energy 302 (2021) 117481.
[28] D.G. Caglayan, H.U. Heinrichs, M. Robinius, D. Stolten, Robust design of a future 100% renewable european energy supply system with hydrogen infrastructure, International Journal of Hydrogen Energy 46(57) (2021) 29376-29390.
[29] M. Hattori, S. Iijima, T. Nakao, H. Hosono, M. Hara, Solid solution for catalytic ammonia synthesis from nitrogen and hydrogen gases at 50° C, Nature communications 11(1) (2020) 1-8.
[30] J.I. Levene, M.K. Mann, R.M. Margolis, A. Milbrandt, An analysis of hydrogen production from renewable electricity sources, Solar energy 81(6) (2007) 773-780.
[31] M. Reuß, T. Grube, M. Robinius, P. Preuster, P. Wasserscheid, D. Stolten, Seasonal storage and alternative carriers: A flexible hydrogen supply chain model, Applied energy 200 (2017) 290-302.
[32] S.D.C. Walsh, L. Easton, Z. Weng, C. Wang, J. Moloney, A. Feitz, Evaluating the economic fairways for hydrogen production in Australia, International Journal of Hydrogen Energy 46(73) (2021) 35985-35996.

[33] P.G. Hartley, V. Au, Towards a Large-Scale Hydrogen Industry for Australia. , 2020. https://www.h2knowledgecentre.com/content/journal2323. Assessed on 1st May 2022.

[34] A.J. Feitz, E. Tenthorey, R. Coghlan, Prospective hydrogen production regions of Australia, Geoscience Australia2019.

[35] M. Li, Y. Bai, C. Zhang, Y. Song, S. Jiang, D. Grouset, M. Zhang, Review on the research of hydrogen storage system fast refueling in fuel cell vehicle, International Journal of Hydrogen Energy 44(21) (2019) 10677-10693.

[36] A. Amid, D. Mignard, M. Wilkinson, Seasonal storage of hydrogen in a depleted natural gas reservoir, International journal of hydrogen energy 41(12) (2016) 5549-5558.

[37] J. Zheng, X. Liu, P. Xu, P. Liu, Y. Zhao, J. Yang, Development of high pressure gaseous hydrogen storage technologies, International Journal of Hydrogen Energy 37(1) (2012) 1048-1057.

[38] CSIRO, Underground Hydrogen Storage in Australia Project, 2021. https://research.csiro.au/hydrogenfsp/our-research/projects/our-research-in-underground-hydrogen-storage-in-australia/. Assessed on 13th Feb 2022.

[39] N. Dopffel, S. Jansen, J. Gerritse, Microbial side effects of underground hydrogen storage–Knowledge gaps, risks and opportunities for successful implementation, International Journal of Hydrogen Energy 46(12) (2021) 8594-8606.

[40] J. Wang, Y. Yang, S. Cai, J. Yao, Q. Xie, Pore-scale modelling on hydrogen transport in porous media: Implications for hydrogen storage in saline aquifers, International Journal of Hydrogen Energy (2023).

[41] U. Bünger, J. Michalski, F. Crotogino, O. Kruck, Large-scale underground storage of hydrogen for the grid integration of renewable energy and other applications, Compendium of hydrogen energy, Elsevier2016, pp. 133-163.

[42] J. Li, Y. Tang, X. Shi, W. Xu, C. Yang, Modeling the construction of energy storage salt caverns in bedded salt, Applied Energy 255 (2019) 113866.

[43] W. Liu, Z. Zhang, J. Chen, D. Jiang, F. Wu, J. Fan, Y. Li, Feasibility evaluation of large-scale underground hydrogen storage in bedded salt rocks of China: A case study in Jiangsu province, Energy 198 (2020) 117348.

[44] A. Craig, S. Newman, P. Stephenson, C. Evans, S. Yancazos, S. Barber, Hydrogen storage potential of depleted oil and gas fields in Western Australia, The APPEA Journal 62(1) (2022) 185-195.

[45] K.M. Jonathan Ennis-King, Julian Strand, Regina Sander, Chris Green, Underground storage of Hydrogen: Mapping out the options for Australia, CSIRO Energy, 2021, p. 95.

[46] S.J.M. Blaber, J.W. Young, M.C. Dunning, Community structure and zoogeographic affinities of the coastal fishes of the Dampier region of north-western Australia, Marine and Freshwater Research 36(2) (1985) 247-266.

[47] P. Haines, The Carribuddy Group and Worral Formation, Canning Basin, Western Australia, Stratigraphy, sedimentology, and petroleum potential Geological Survey of Western Australia. Report 105 60p (2009).

[48] D.A. McNaughton, T. Quinlan, R. Hopkins, A. Wells, Evolution of salt anticlines and salt domes in the Amadeus Basin, central Australia, Geological Society of America, Special Paper 88 (1968) 229-247.

[49] P.W. Haines, The Carribuddy Group and Worral Formation, Canning Basin, Western Australia: Stratigraphy, Sedimentology, and Petroleum Potential, Geological Survey of Western AustraliaReport 105, 2009.

[50] A. Feitz, E. Tenthorey, R. Coghlan, Prospective hydrogen production regions of Australia. Record 2019/15, Geoscience Australia: Canberra (2019).

[51] P. Li, Y. Li, X. Shi, A. Zhao, S. Hao, X. Gong, S. Jiang, Y. Liu, Stability analysis of U-shaped horizontal salt cavern for underground natural gas storage, Journal of Energy Storage 38 (2021) 102541.

[52] D. Evans, D. Parkes, M. Dooner, P. Williamson, J. Williams, J. Busby, W. He, J. Wang, S. Garvey, Salt Cavern Exergy Storage Capacity Potential of UK Massively Bedded Halites, Using Compressed Air Energy Storage (CAES), Applied Sciences 11(11) (2021) 4728.

[53] H. Yin, C. Yang, H. Ma, X. Shi, N. Zhang, X. Ge, H. Li, Y. Han, Stability evaluation of underground gas storage salt caverns with micro-leakage interlayer in bedded rock salt of Jintan, China, Acta Geotechnica 15(3) (2020) 549-563.

[54] M. Cała, K. Cyran, M. Kowalski, P. Wilkosz, Influence of the anhydrite interbeds on a stability of the storage caverns in the Mechelinki salt deposit (Northern Poland), Archives of Mining Sciences (2018) 1007-1025-1007-1025.

[55] P. Bérest, A. Réveillère, D. Evans, M. Stöwer, Review and analysis of historical leakages from storage salt caverns wells, Oil & Gas Science and Technology–Revue d'IFP Energies nouvelles 74 (2019) 27.

[56] E. Fichtner, Erstellung eines entwicklungskonzeptes energiespeicher in niedersachsen, Fichtner GmbH & Co. KG Stuttgart, Germany, 2014.

[57] H. Blanco, A. Faaij, A review at the role of storage in energy systems with a focus on Power to Gas and long-term storage, Renewable and Sustainable Energy Reviews 81 (2018) 1049-1086.

[58] H. Stille, The upthrust of the salt masses of Germany, AAPG Bulletin 9(3) (1925) 417-441.

[59] M.C. Geluk, Stratigraphy and tectonics of Permo-Triassic basins in the Netherlands and surrounding areas, Utrecht University2005.

[60] D.G. Caglayan, N. Weber, H.U. Heinrichs, J. Linßen, M. Robinius, P.A. Kukla, D. Stolten, Technical potential of salt caverns for hydrogen storage in Europe, International Journal of Hydrogen Energy 45(11) (2020) 6793-6805.

[61] G. Australia, Applying geoscience to Australia's most important challenges 2022 https://www.ga.gov.au/scientific-topics/energy/resources/hydrogen. Assessed on 13th Feb 2022.

[62] R.J. Korsch, J. Kennard, Geological and geophysical studies in the Amadeus Basin, central Australia, Bureau of Mineral Resources, Geology and Geophysics1991.

[63] J.F. Lindsay, Upper Proterozoic evaporites in the Amadeus basin, central Australia, and their role in basin tectonics, Geological Society of America Bulletin 99(6) (1987) 852-865.

[64] P.W. Haines, H.J. Allen, K. Grey, The Amadeus Basin in Western Australia: a forgotten corner of the Centralian Superbasin, Geological Survey of Western Australia Annual Review (2008-2009) 49-57.

[65] C. Edgoose, M. Ahmad, Geology and mineral resources of the Northern Territory. Northern Territory geological survey special publication 5, (2013).

[66] AusH2, AusH2 - Australia's Hydrogen Opportunities Tool. https://portal.ga.gov.au/persona/hydrogen. Assessed on 19/04/2021, 2021. https://portal.ga.gov.au/persona/hydrogen. (Accessed 19/04/2021.

[67] V.M. Kovalevych, W.-L. Zang, T. Peryt, O.V. Khmelevska, S. Halas, I. Iwasinska-Budzyk, P.J. Boult, P.S. Heithersay, Deposition and chemical composition of Early Cambrian salt in the eastern Officer Basin, South Australia, Australian Journal of Earth Sciences 53(4) (2006) 577-593.

[68] A. Simeonova, R. Iasky, Salt tectonics in the Officer Basin: implications for trap formation and petroleum exploration, ASEG Extended Abstracts 2004(1) (2004) 1-4.

[69] J.N. Dunster, Sedimentology of the Ouldburra formation (Early Cambrian), northeastern Officer Basin, 1987.

[70] A.P. Simeonova, N. Apak, Salt deformation and associated traps, Officer Basin, Western Australia, AAPG International Conference Barcelona, Spain September, 2003, pp. 21-24.

[71] N. Zhang, X. Shi, Y. Zhang, P. Shan, Tightness analysis of underground natural gas and oil storage caverns with limit pillar widths in bedded rock salt, Ieee Access 8 (2020) 12130-12145.

[72] J. Chen, S. Ren, C. Yang, D. Jiang, L. Li, Self-healing characteristics of damaged rock salt under different healing conditions, Materials 6(8) (2013) 3438-3450.

[73] J.W. Snedden, P.J. Vrolijk, L.T. Sumpter, M.L. Sweet, K.R. Barnes, E. White, M.E. Farrell, Reservoir connectivity: definitions, examples, and strategies, IPTC 2007: International Petroleum Technology Conference, European Association of Geoscientists & Engineers, 2007, pp. cp-147-00089.

[74] T.J. Parker, A.N. McDowell, Model studies of salt-dome tectonics, AAPG Bulletin 39(12) (1955) 2384-2470.

[75] Q. Wanyan, G. Ding, Y. Zhao, K. Li, J. Deng, Y. Zheng, Key technologies for salt-cavern underground gas storage construction and evaluation and their application, Natural Gas Industry B 5(6) (2018) 623-630.
[76] L. Zeng, M. Hosseini, A. Keshavarz, S. Iglauer, Y. Lu, Q. Xie, Hydrogen wettability in carbonate reservoirs: Implication for underground hydrogen storage from geochemical perspective, International Journal of Hydrogen Energy 47(60) (2022) 25357-25366.
[77] L. Zeng, A. Keshavarz, N.K. Jha, A. Al-Yaseri, M. Sarmadivaleh, Q. Xie, S. Iglauer, Geochemical Modelling of Hydrogen Wettability on Quartz: Implications for Underground Hydrogen Storage in Sandstone Reservoirs, Journal of Molecular Liquids (2022) 121076.
[78] L. Zeng, A. Keshavarz, Q. Xie, S. Iglauer, Hydrogen storage in Majiagou carbonate reservoir in China: Geochemical modelling on carbonate dissolution and hydrogen loss, International Journal of Hydrogen Energy 47(59) (2022) 24861-24870.
[79] L. Zeng, M. Sarmadivaleh, A. Saeedi, A. Al-Yaseri, C. Dowling, G. Buick, Q. Xie, Thermodynamic Modelling on Wellbore Cement Integrity During Underground Hydrogen Storage in Depleted Gas Reservoirs, SPE Asia Pacific Oil & Gas Conference and Exhibition, OnePetro, 2022.
[80] A. Aftab, A. Hassanpouryouzband, Q. Xie, L.L. Machuca, M. Sarmadivaleh, Toward a Fundamental Understanding of Geological Hydrogen Storage, Industrial & Engineering Chemistry Research 61(9) (2022) 3233-3253.
[81] Y. Li, X. Chen, X. Shi, N. Zhang, C. Ma, C. Yang, Analysis of the plugging process of the leaking interlayer in a thin interbedded salt cavern gas storage of Jintan (China) by high-pressure grouting and potential applications, Journal of Natural Gas Science and Engineering 68 (2019) 102918.

[82] D. Remus, K. Tindale, The Pleasant Creek Arch, Adavale Basin, a Mid Devonian to Mid Carboniferous thrust system, The APPEA Journal 28(1) (1988) 208-216.

[83] A. Troup, B. Talebi, Adavale Basin petroleum plays, The APPEA Journal 59(2) (2019) 958-964.

[84] R. Paten, The Adavale Basin Queensland, (1977).

[85] G.W. Gill, Storage: Optimising power generation assets using underground salt caverns, Energy News 33(3) (2015) 15.

[86] P. Lehmann, The stratigraphy, palaeogeography and petroleum potential of the Lower to lower Upper Devonian sequence in the Canning Basin, (1984).

[87] D.L. Cathro, J.K. Warren, G.E. Williams, Halite saltern in the Canning Basin, Western Australia: a sedimentological analysis of drill core from the Ordovician-Silurian Mallowa Salt, Sedimentology 39(6) (1992) 983-1002.

[88] WAPIMS, Petroleum & Geothermal Information Management System. https://wapims.dmp.wa.gov.au/WAPIMS/ Assessed on 14th May 2022., 2022.

[89] G. WA, GEOVIEW WA. https://geoview.dmp.wa.gov.au/geoview/?Viewer=GeoView. Assessed on 1st May 2022, 2022.

[90] K.M. Jonathan Ennis-King, Julian Strand, Regina Sander, Chris Green, Underground storage of hydrogen: mapping out the options for Australia, Australia, 2021, p. 95.

[91] S.T. Brennan, T.K. Lowenstein, The major-ion composition of Silurian seawater, Geochimica et Cosmochimica Acta 66(15) (2002) 2683-2700.

[92] P.W. Haines, Geological appraisal of petroleum exploration well Patience 2, Canning Basin, Western Australia, Geological Survey of Western AustraliaReport number 2011/11, 2012.

[93] P. Haines, H.-J. Allen, Hydrocarbon and helium prospectivity of the Amadeus and Murraba basins in Western Australia, (2019).

[94] G. Gill, G. Cowan, Advale Basin, Queensland Underground Salt Cavern Storage Potenial, 2021. https://www.yumpu.com/en/document/read/39912073/adavale-basin-salt-cavern-storage-potential-innovative-energy-. Assessed on 13th Feb 2022. (Accessed 19/04/2021.

[95] I. Contrucci, E. Klein, P. Bigarré, A. Lizeur, A. Lomax, M. Bennani, Management of post-mining large-scale ground failures: blast swarms field experiment for calibration of permanent microseismic early-warning systems, Pure and applied geophysics 167(1) (2010) 43-62.

[96] A. Ozarslan, Large-scale hydrogen energy storage in salt caverns, International journal of hydrogen energy 37(19) (2012) 14265-14277.

[97] T. Wang, C. Yang, H. Ma, J.J.K. Daemen, H. Wu, Safety evaluation of gas storage caverns located close to a tectonic fault, Journal of Natural Gas Science and Engineering 23 (2015) 281-293.

[98] R. Span, E.W. Lemmon, R.T. Jacobsen, W. Wagner, A. Yokozeki, A reference equation of state for the thermodynamic properties of nitrogen for temperatures from 63.151 to 1000 K and pressures to 2200 MPa, Journal of Physical and Chemical Reference Data 29(6) (2000) 1361-1433.

[99] E.W. Lemmon, R.T. Jacobsen, Viscosity and thermal conductivity equations for nitrogen, oxygen, argon, and air, International journal of thermophysics 25(1) (2004) 21-69.

[100] J.W. Leachman, R.T. Jacobsen, S. Penoncello, E.W. Lemmon, Fundamental equations of state for parahydrogen, normal hydrogen, and orthohydrogen, Journal of Physical and Chemical Reference Data 38(3) (2009) 721-748.

[101] C.D. Muzny, M.L. Huber, A.F. Kazakov, Correlation for the viscosity of normal hydrogen obtained from symbolic regression, Journal of Chemical & Engineering Data 58(4) (2013) 969-979.

[102] U. Setzmann, W. Wagner, A new equation of state and tables of thermodynamic properties for methane covering the range from the melting line to 625 K at pressures up to 1000 MPa, Journal of Physical and Chemical reference data 20(6) (1991) 1061-1155.

[103] I.H.B. Eric W. Lemmon, Marcia L. Huber, and Mark O. McLinden, "Thermophysical Properties of Fluid Systems" in NIST Chemistry WebBook, NIST Standard Reference Database Number 69 Eds. P.J. Linstrom and W.G. Mallard, National Institute of Standards and Technology, Gaithersburg MD, 20899, https://doi.org/10.18434/T4D303, Assessed on 16th April, 2022.

[104] C. Hemme, W. van Berk, Potential risk of H2S generation and release in salt cavern gas storage, Journal of Natural Gas Science and Engineering 47 (2017) 114-123.

[105] S. Donadei, G.-S. Schneider, Chapter 6 Compressed air energy storage in underground formations, Storing Energy, Elsevier2016, pp. 113-133.

[106] F. Crotogino, Traditional Bulk Energy Storage—Coal and Underground Natural Gas and Oil Storage, Storing Energy, Elsevier2016, pp. 391-409.

[107] W. Colella, M. Jacobson, D. Golden, Switching to a US hydrogen fuel cell vehicle fleet: The resultant change in emissions, energy use, and greenhouse gases, Journal of Power Sources 150 (2005) 150-181.

[108] E. ToolBox, Circles within a Rectangle - Calculator. https://www.engineeringtoolbox.com/circles-within-rectangle-d_1905.html. Assessed on 14th May 2022, 2022.

[109] A. Hassanpouryouzband, E. Joonaki, K. Edlmann, N. Heinemann, J. Yang, Thermodynamic and transport properties of hydrogen containing streams, Scientific Data 7(1) (2020) 1-14.

[110] A. Hassanpouryouzband, E. Joonaki, K. Edlmann, R.S. Haszeldine, Offshore geological storage of hydrogen: Is this our best option to achieve net-zero?, ACS Energy Letters 6(6) (2021) 2181-2186.

[111] C.S. Association, Storage of hydrocarbons in underground formations: Z341 Series-10, Canadian Standards Association, Mississauga, Ontario, Canada (2006).

[112] K. DeVries, Improved modeling increases salt cavern storage working gas, GasTIPS 9(1) (2003) 33-36.

[113] T. Wang, J. Li, G. Jing, Q. Zhang, C. Yang, J.J. Daemen, Determination of the maximum allowable gas pressure for an underground gas storage salt cavern–A case study of Jintan, China, Journal of Rock Mechanics and Geotechnical Engineering 11(2) (2019) 251-262.

[114] S. Yildirim, Consideration of the mechanical damage behavior of rock salt during calculation of infiltration-cracks in the edge zone of gas storage caverns, IOP Conference Series: Earth and Environmental Science, IOP Publishing, 2021, p. 012183.

[115] H. Reward, 2008 Annual Report Canning Basin, 2008, p. 6.

[116] X.-S. Chen, Y.-P. Li, Y.-L. Jiang, Y.-X. Liu, T. Zhang, Theoretical research on gas seepage in the formations surrounding bedded gas storage salt cavern, Petroleum Science (2022).

[117] D. Wei, D. Qu, Y. Pei, SY6806-2010 Safety rules of salt cavern underground gas storage [S], Bei Jing: Petroleum Industry Press, 2011.

[118] J. Begg, Structuring and controls on Devonian reef development on the north-west Barbwire and adjacent terraces, Canning Basin, The APPEA Journal 27(1) (1987) 137-151.

[119] Y. Zhan, A seismic interpretation of the Broome Platform, Willara Sub-basin and Munro Arch of the Canning Basin, Western Australia, Geological Survey of Western Australia (2019).

[120] Y. Zhan, Seismic interpretation of salt occurrences in the southern Canning Basin, Western Australia, (2019).

[121] A. Energy, Australian Energy Update 2020 2020. https://www.energy.gov.au/sites/default/files/Australian%20Energy%20Statistics%20 2020%20Energy%20Update%20Report_0.pdf. Assessed on 3rd Sept, 2021.